(12) INTERNATIONAL APPLICATION PUBLISHED UNDER THE PATENT COOPERATION TREATY (PCT)

(19) World Intellectual Property Organization
International Bureau

(43) International Publication Date
17 October 2013 (17.10.2013)

WIPO | PCT

(10) International Publication Number
WO 2013/154587 A1

(51) **International Patent Classification**:
C07K 1/00 (2006.01) ***C12N 5/00*** (2006.01)
C07H 21/04 (2006.01)

(21) **International Application Number**:
PCT/US2012/033639

(22) **International Filing Date**:
13 April 2012 (13.04.2012)

(25) **Filing Language**: English

(26) **Publication Language**: English

(71) **Applicants** *(for all designated States except US)*: **CENTRO DE ESTUDIOS CIENTIFICOS DE VALDIVIA** [CL/CL]; Arturo Prat 514, Valdivia (CL). **CARNEGIE, INSTITUTION OF WASHINGTON** [US/US]; 1530 P Street, N.W., Washington, DC 20005 (US).

(72) **Inventors; and**

(75) **Inventors/Applicants** *(for US only)*: **BARROS OLMEDO, Luis Felipe** [CL/CL]; Arturo Prat 514, Valdivia (CL). **SAN MARTIN, Alejandro** [CL/CL]; Arturo Prat 514, Valdivia (CL). **CEBALLO CHARPENTIER, Sebastian** [CL/CL]; Arturo Prat 514, Valdivia (CL). **FROMMER, Wolf, B.** [DE/US]; 1530 P Street, N.W., Washington, DC 20005 (US).

(74) **Agent**: **DEMASTER, Eric, E.**; Merchant & Gould P.C., P.o. Box 2903, Minneapolis, MN 55402-0903 (US).

(81) **Designated States** *(unless otherwise indicated, for every kind of national protection available)*: AE, AG, AL, AM, AO, AT, AU, AZ, BA, BB, BG, BH, BR, BW, BY, BZ, CA, CH, CL, CN, CO, CR, CU, CZ, DE, DK, DM, DO, DZ, EC, EE, EG, ES, FI, GB, GD, GE, GH, GM, GT, HN, HR, HU, ID, IL, IN, IS, JP, KE, KG, KM, KN, KP, KR, KZ, LA, LC, LK, LR, LS, LT, LU, LY, MA, MD, ME, MG, MK, MN, MW, MX, MY, MZ, NA, NG, NI, NO, NZ, OM, PE, PG, PH, PL, PT, QA, RO, RS, RU, RW, SC, SD, SE, SG, SK, SL, SM, ST, SV, SY, TH, TJ, TM, TN, TR, TT, TZ, UA, UG, US, UZ, VC, VN, ZA, ZM, ZW.

(84) **Designated States** *(unless otherwise indicated, for every kind of regional protection available)*: ARIPO (BW, GH, GM, KE, LR, LS, MW, MZ, NA, RW, SD, SL, SZ, TZ, UG, ZM, ZW), Eurasian (AM, AZ, BY, KG, KZ, MD, RU, TJ, TM), European (AL, AT, BE, BG, CH, CY, CZ, DE, DK, EE, ES, FI, FR, GB, GR, HR, HU, IE, IS, IT, LT, LU, LV, MC, MK, MT, NL, NO, PL, PT, RO, RS, SE, SI, SK, SM, TR), OAPI (BF, BJ, CF, CG, CI, CM, GA, GN, GQ, GW, ML, MR, NE, SN, TD, TG).

Published:

— *with international search report (Art. 21(3))*

— *with sequence listing part of description (Rule 5.2(a))*

WO 2013/154587 A1

(54) **Title**: GENETICALLY ENCODED PROBE FOR QUANTIFICATION OF LACTATE, AND METHODS FOR QUANTIFYING METABOLIC RATES AND LACTATE TRANSPORT

(57) **Abstract**: A nanosensor for detecting and quantifying lactate in different types of samples, such as tissues, intra-cellular and subcellular compartments, with high spatial and temporal resolution is disclosed. Methods comprising use of the nanosensor for quantifying the activity of lactate transporters, rates of cellular lactate production and cellular lactate consumption, and rate of mitochondrial pyruvate consumption are also disclosed. Methods for quantifying the transformation in energy metabolism that characterizes cancer cells with single-cell resolution and for detecting interference of candidate drugs with mitochondrial energetics are additionally disclosed.

GENETICALLY ENCODED PROBE FOR QUANTIFICATION OF LACTATE, AND METHODS FOR QUANTIFYING METABOLIC RATES AND LACTATE TRANSPORT

This application is being filed on 13 April 2012, as a PCT International Patent application in the name of Centro de Estudios Cientificos de Valdivia a Chilean corporation and Carnegie Institution of Washington, a U.S. national corporation, applicant for the designation of all countries except the US, and Luis Felipe Barros Olmedo, Alejandro San Martin, Sebastian Ceballo Charpentier, all citizens of Chile, and Wolf B. Frommer, a citizen of Germany, applicants for the designation of the US only.

FIELD OF THE INVENTION

The present invention comprises a nanosensor for detecting and quantifying lactate in different types of samples, such as tissues, intra-cellular and even in subcellular compartments, with high spatial and temporal resolution, across four orders of concentration magnitude, and methods that make use of this nanosensor for the quantification of the activity of lactate transporters, for the quantification of the rates of cellular lactate production and cellular lactate consumption, and for the quantification of the rate of mitochondrial pyruvate consumption. Additionally, the invention comprises a method to quantify the transformation in energy metabolism that characterizes cancer cells with single-cell resolution and a method to detect interference of candidate drugs with mitochondrial energetics.

BACKGROUND OF THE INVENTION

Lactate is an organic chemical compound that participates in the metabolism of eukaryotic and prokaryotic cells. Lactate is exchanged between organelles, cells and organs as fuel or waste product, and also plays important signaling and biosynthetic roles, being involved in the physiology of exercise, inflammation, wound healing, neurovascular coupling and also in diseases such as cancer, hypoxic/ischemic disease and microbial infection. In addition, lactate is of industrial interest as a food

additive, as a detergent, for the detection and control of microbial growth and for the production of biodegradable polymers.

Lactate is in dynamic flux between subcellular compartments, between the cell and the extracellular space and between cells. Because the concentration of lactate in the cell compartments is unknown, the dynamics of lactate in the living body is a largely unknown area.

Standard methods to measure lactate are based on enzymatic reactions, which have to be followed by photometric, amperometric or other devices. Enzyme-based electrodes have been developed that can detect lactate with high-temporal resolution. Another approach to measure lactate is high performance liquid chromatography (HPLC), where lactate is separated from other compounds by passing the sample through a stationary phase stored in a column. There is a problem in the prior art, however, that the existing methods are invasive as they require the extraction of samples or consume lactate, and therefore, they change the concentration of lactate in the sample. A second problem is their sensitivity, since they can not detect the minute amount of lactate present in a single cell or a single subcellular organelle.

The transport of lactate across cellular and subcellular membranes is mediated by the monocarboxylate transporter (MCT), a molecule involved in the pathogenesis of several diseases and an important target for pharmacological intervention in cancer and diabetes. There are no available methods to measure the transport of lactate in single cells. More specifically, current and common techniques used to measure the transport of lactate using radioactive isotopes cannot resolve single cells and have poor temporal resolution, which hampers the study of fast phenomena and normal tissues, which are heterogeneous in their cellular composition. An existing technique infers the transport of lactate in single cells from changes in pH that accompany the transport of lactate, but this technique is limited insofar as requires prior knowledge of the usually unknown buffering capacity of the cell and is not easily applicable in the presence of physiological bicarbonate buffers.

The rates of lactate production and lactate consumption are important parameters of cell metabolism, with relevance for hypoxia/ischemia, cancer, diabetes and other pathological conditions. There are no available methods to measure the rates of lactate production and consumption in single cells. More

specifically, current and common techniques used to measure the rates of lactate production and consumption are enzyme-based methods that cannot resolve single cells, have poor temporal resolution, and cannot be applied in the presence of physiological concentrations of lactate. Particularly, measurements using isotopes cannot resolve single cells and have poor sensitivity and temporal resolution. Other currently available technique infers the production of lactate by a cell population by following changes in pH that accompany the production of lactate, but this indirect technique is limited insofar as it is affected by other mechanisms affecting extracellular pH and is not easily applicable in the presence of physiological bicarbonate buffers.

The rate of pyruvate consumption by mitochondria, equivalent under some conditions to the rate of the tricarboxylic acid (TCA) cycle and oxidative phosphorylation, is one of the fundamental parameters of cell metabolism and is affected in several diseases including hypoxic/ischemia, cancer, diabetes and other conditions. There are no available methods to measure the rates of the mitochondrial metabolism in single cells. More specifically, current and common techniques to measure the rates of the mitochondrial metabolism use cannot resolve single cells and have poor sensitivity and low temporal resolution.

In the state of the art there is no evidence of an optical tool or nanosensor for detecting and quantifying lactate in samples, in tissues and in cellular and subcellular compartments, with high spatial and temporal resolution. Also, there are no available techniques to quantitate single-cell resolution lactate transport or the rates of lactate consumption/production or the rate of mitochondrial metabolism or the Warburg effect, the metabolic transformation that underlies cancer. Nevertheless there are related documents in the art, which will be described below.
Sensors for different metabolites are described in WO2006096213A1, WO2006096214A1, WO2006044612A2 and WO2007046786A2 that involve a FRET donor, a FRET acceptor and a member of the class of periplasmic binding proteins (PBPs), proteins located in outside bacterial plasma membranes involved in chemotaxis. The periplasmic binding protein serves as the specific recognition element. As there is no known rule to predict whether a given protein may serve as an effective recognition element, these proteins have been the result of informed trial and error, semi-rational design. The current invention does not used any of the

recognition elements described WO2006096213A1, WO2006096214A1, WO2006044612A2 or WO2007046786A2. Moreover, the current invention is not based on any members of the periplasmic binding protein family but rather on a member of the GntR family, a subclass of transcription factors involved in adaptation of bacteria to changing environmental conditions. Surprisingly, the sensor described in the present invention was found to detect its ligand over 4 orders of magnitude, which makes it unique. PBP-based sensors can only quantify ligands over 2 orders of magnitude only.

WO2001033199A2 discloses a probe based on a target binding site peptide (i) attached to a first fluorescent polypeptide capable of binding to (i) and attached to a second fluorescent polypeptide. The probe includes a linker connecting the two fluorescent polypeptides which allows the distance between them to vary, the fluorescent polypeptides display fluorescence resonance energy transfer (FRET) between them. The probe described in WO2001033199A2 is qualitatively different from the probe described in the current invention insofar as the current invention does not involve displacement of binding between two peptides but rather a conformational change elicited by the ligand in a whole protein.

WO2008008149 describes a method to measure the rates of glycolysis and mitochondrial metabolism in cell populations by recording the rate of extracellular oxygen depletion and the rate of extracellular acidification over minutes using a specific dedicated apparatus. The current invention differs from WO2008008149 as it does not need a dedicated apparatus and can be used with standard multi-well plate readers. It also differs in terms of spatial resolution as it can measure single cells and temporal resolution, which is in the order of seconds. The current invention measures the rate of lactate production directly, whereas WO2008008149 provides an indirect estimate by recording the accumulation of extracellular protons, a parameter that is affected by other processes unrelated to metabolism and that required unphysiological pH buffering conditions.

WO/2012/002963 describes a method to estimate the rate of glucose consumption in single cells or cell population with high temporal resolution using a FRET glucose nanosensor. The current invention differs from WO/2012/002963 as is does not measure glucose or the rate of glucose consumption but the rates of lactate production/consumption and the rate of mitochondrial metabolism, rates that

are independent of the rate of glucose consumption, being a completely different technical application. Moreover, the present method allows an estimation of the Warburg effect, which is not possible with a glucose nanosensor.

DISCLOSURE OF THE INVENTION

The subject of the present invention is to provide a nanosensor, which allows minimally-invasive measurement of lactate over an extended range of lactate concentration with high sensitivity regardless of the concentration of the probe, which does not consume lactate during measurement, and that can be used to measure lactate in samples, in cells and in subcellular compartments. Further, the subject of the present invention is to provide a measuring method of lactate using the nanosensor. Said method can be used to measure the activity of the lactate transporters, to measure the rates of cellular lactate production and lactate consumption, and to measure the rate of pyruvate consumption by mitochondria, which under certain conditions is equivalent to the rate of the tricarboxylic acid (TCA) cycle, a method for single-cell quantification of the Warburg effect, a transformation of metabolism that characterizes cancer cells, and a method to detect interference between drugs and bioenergetic pathways.

BRIEF DESCRIPTION OF THE INVENTION

The present invention is related to a genetically-encoded Forster resonance energy transfer (FRET)-based indicator composed of the bacterial LldR transcription factor sandwiched between any suitable donor and acceptor fluorescent proteins moieties that are capable in combination of serving as donor and acceptor moieties in FRET. Preferred donor and acceptor moieties are selected from the group consisting of mTFP (monomeric teal fluorescent protein), CFP (cyan fluorescent protein), BFP (blue fluorescent protein), GFP (green fluorescent protein), YFP (yellow fluorescent protein), enhanced variations thereof such as enhanced YFP (EYFP), Citrine or Venus, or infrared fluorescent proteins from bacterial phytochromes, with a particularly preferred embodiment provided by the donor/acceptor mTFP/YFP Venus, a variant of YFP with improved pH tolerance and maturation time (Nagai et al., 2002). Criteria to consider when selecting donor and acceptor fluorescent moieties is known in the art, for instance as disclosed in U.S.

Pat. No 6,197, 928, which is herein incorporated by reference in its entirety. An alternative is the use of a single fluorescent moiety such as circularly-permuted variations of GFP (Akerboom et al., 2008) inserted into the backbone of LldR or other suitable lactate-binding protein, which undergoes a change in fluorescence intensity in response to binding of lactate to the LldR moiety or to other suitable lactate-binding protein. In a more preferred embodiment, the fluorescent proteins are mTFP and Venus.

Unexpectedly, the lactate sensor of the present invention shows a biphasic dose response curve with apparent dissociation constants for lactate of 8 μM and 800 μM, which allows quantitation of lactate over four orders of magnitude (from 10^{-6} to 10^{-2} M), and differs from all existing FRET metabolite nanosensors, which only allow measurement over two orders of magnitude, for example WO2006096213A1, WO2006096214A1, WO2006044612A2 and WO2007046786A2. The invention also comprises methods that exploit the high spatiotemporal resolution of the lactate sensor of the present invention for the measurement of lactate, which, depending on the configuration of the method, allows the measurement of transport activity and of two metabolic rates, the rate of lactate production/consumption and the rate of pyruvate consumption by mitochondria and a method to quantify the Warburg phenomenon in single-cells. These methods can be applied to single cells or cell populations, adherent cells or in suspension, to a cell culture, a tissue culture, a mixed cell culture, a tissue explant, or it can also be applied to animal tissues *in vivo*. The method comprises the expression of the lactate sensor of the present invention in individual cells.

The nanosensor of the present invention is expressed in single cells or cell populations, adherent cells or in suspension, in a cell culture, a tissue culture, a mixed cell culture, a tissue explant, or in animal tissues *in vivo*. The gene expression can be attained by any suitable method to transfer the sensor gene information to the host cell. Examples of gene transfer methodologies are plasmid transfer for instance using liposomal delivery, virus transfer and transgenesis.

Once the sensor is expressed in single cells or cell populations, adherent cells or in suspension, in a cell culture, a tissue culture, a mixed cell culture, a tissue explant, or in animal tissues *in vivo*, the sensor is calibrated according to pre-

established conditions. In order to express fluorescence data in terms of lactate concentration, a single-point calibration protocol is applied at the end of each experiment. Briefly, intracellular lactate is first lowered by depriving the cells of lactate and glucose, a maneuver that inhibits lactate production at Lactate dehydrogenase (LDH). To ensure that cytosolic lactate is indeed negligible, cells are exposed to pyruvate, which on entering via MCT, increases in the number of inward-facing binding sites available for lactate extrusion, effectively "pumping out" the residual lactate. With the value for the fluorescence ratio at this "zero" lactate condition, the kinetic constants determined in vitro, and the maximum change of fluorescence ratio of 38% or the value determined for a each cell type, fluorescence data are converted into lactate concentration as shown in Fig. 12.

The nanosensor of the invention, is further used in a method for determination of lactate concentrations as described before in single cells or cell populations, adherent cells or in suspension, in a cell culture, a tissue culture, a mixed cell culture, a tissue explant, or in animal tissues *in vivo*.
Depending on the configuration of the method for determination of lactate concentrations, in a first embodiment, the use of the nanosensor of the invention, in a method allows the determination of the lactate transporter activity (i.e. estimation of kinetic parameters of lactate transporter).

In a second embodiment, the use of the nanosensor of the invention, in a method allows determination of lactate production and/or consumption rates.

In a third embodiment, the use of the nanosensor of the invention, in a method allows the measurement of mitochondrial pyruvate consumption and/or production rates.

In a further embodiment, the use of the nanosensor of the invention, in a method for single-cell quantification of the Warburg effect.

Both the foregoing summary and the following detailed description provide examples and are explanatory only. Accordingly, the foregoing summary and the following detailed description should not be considered to be restrictive. Further, features or variations may be provided in addition to those set forth herein. For example, certain embodiments may be directed to various feature combinations and sub-combinations described in the detailed description.

BRIEF DESCRIPTION OF THE DRAWINGS

The invention is illustrated by the accompanying drawings wherein:

Figure 1 shows the tridimensional structures of the transcriptional regulator LldR from *E. coli* and *C. glutamicum.*

Figure 2 shows the amino acid sequences of LldR from *E. coli* and *C. glutamicum.*

Figure 3 shows the alignment of the amino acid sequences of sixteen variants of the lactate sensor, SEQ ID NO 1 corresponding to variant 1, SEQ ID NO 2 corresponding to variant 2, SEQ ID NO 3 corresponding to variant 3, SEQ ID NO 4 corresponding to variant 4, SEQ ID NO 5 corresponding to variant 5, SEQ ID NO 6 corresponding to variant 6, SEQ ID NO 7 corresponding to variant 7, SEQ ID NO 8 corresponding to variant 8, SEQ ID NO 9 corresponding to variant 9, SEQ ID NO 10 corresponding to variant 10, SEQ ID NO 11 corresponding to variant 11, SEQ ID NO 12 corresponding to variant 12, SEQ ID NO 13 corresponding to variant 13, SEQ ID NO 14 corresponding to variant 14, SEQ ID NO 15 corresponding to variant 15, SEQ ID NO 16 corresponding to variant 16.

Figure 4 shows the response to lactate of sixteen variants of the lactate sensor, wherein the black filled bars correspond to the variants 1, 3, 5, 7, 9, 11, 13, 15, and the grey filled bars correspond to variants 2, 4, 6, 8, 10, 12, 14, and 16.

Figure 5 shows the effect of lactate on the fluorescence emission spectrum of the most responsive variant of the sensor, Variant 7, which is encoded by SEQ ID NO 7.

Figure 6 presents the change in fluorescence ratio of Variant 7, , in response to increasing concentrations of lactate.

Figure 7 summarizes the effect of several molecules on the fluorescence ratio of Variant 7, showing the specificity of the nanosensors.

Figure 8 shows the effect of pH on the fluorescence ratio of the lactate sensor of the present invention.

Figure 9 shows the effect of extracellular lactate on the fluorescence ratio of Variant 7, expressed in HEK293 cells and astrocytes.

Figure 10 shows that sensor concentration does not affect the response of Variant 7, to lactate.

Figure 11 shows the emission spectra and dose-response of Variant 7, encoded by SEQ ID NO 1, expressed in HEK293 cells.

Figure 12 illustrates a one-point calibration protocol for Variant 7, encoded by SEQ ID NO 1.

Figure 13 compares the uses of lactate and pH measurements for the characterization of the lactate transporter in astrocytes.

Figure 14 depicts the main biochemical pathways for lactate in mammalian cells.

Figure 15 demonstrates the measurement of cellular lactate production rate and mitochondrial pyruvate consumption rate in single astrocytes and HEK293 cells.

Figure 16 compares metabolic rates measured experimentally with those obtained by fitting a mathematical model to the data. In the equation shown in Figure 16:

Pyruvate concentration, [Pyr] (μM)

Lactate, [Lac] (μM)

Glycolytic pyruvate production, G (μM/s)

Lactate dexydrogenase forward reaction, LDHf (s-1)

Lactate dehydrogenase reverse reaction, LDHr (s-1)

Cellular lactate release, MCT (μM/s)

Mitochondrial pyruvate uptake, PT (μM/s)

Figure 17 shows the acute activation of lactate production by inhibition of oxidative phosphorylation.

Figure 18 shows the effect of lactate on Variant 7, expressed in T98G glioma cells.

Figure 19 plots the lactate production rate and mitochondrial metabolism in individual astrocytes, HEK293 cells and T98G glioma cells.

Figure 20 shows the Warburg Index of astrocytes and glioma cells.

DETAILED DESCRIPTION OF THE INVENTION

The following detailed description refers to the accompanying drawings. While embodiments of the nanosensor of the invention may be described, modifications, adaptations, and other implementations are possible. For example, substitutions, additions, or modifications may be made to the elements illustrated in

the drawings, and the methods described herein may be modified by substituting, reordering, or adding stages to the disclosed methods. Accordingly, the following detailed description does not limit the scope of the invention. While the nanosensor and the methods are described in terms of "comprising" various elements or steps, the nanosensor and the methods can also "consist essentially of" or "consist of" the various elements or steps, unless stated otherwise. Additionally, the terms "a," "an," and "the" are intended to include plural alternatives, e.g., at least one, unless stated otherwise.

The nanosensor quantifies lactate between 1 μM and 10 mM, allowing single-cell measurement of lactate concentration, lactate transporter (MCT) activity, lactate production and the rate of mitochondrial metabolism, as well as detection of the Warburg effect in individual cells.

The nanosensor of the present invention is a Forster Resonance Energy Transfer (FRET)-based lactate nanosensor further based on LldR, a bacterial transcription regulator that has two modules, a lactate-binding/regulatory domain and a DNA-binding domain. The LldR genes were selected from *Corynebacterium glutamicum* and from *Escherichia coli*.

The tridimensional structure of the two proteins is virtually superimposable (Fig. 1), yet they are only 19.4% identical, differing in numerous charged residues (Fig. 2), which may alter surface charge scanning and possibly FRET efficiency. The FRET-based lactate nanosensor of the invention may incorporate any suitable donor and acceptor fluorescent proteins moieties that are capable in combination of serving as donor and acceptor moieties in FRET. Preferred donor and acceptor moieties are selected from the group consisting of mTFP (monomeric teal fluorescent protein), CFP (cyan fluorescent protein), BFP (blue fluorescent protein), GFP (green fluorescent protein), YFP (yellow fluorescent protein), enhanced variations thereof such as enhanced YFP (EYFP), Citrine or Venus, or infrared fluorescent proteins from bacterial phytochromes, with a particularly preferred embodiment provided by the donor/acceptor mTFP/YFP Venus, a variant of YFP with improved pH tolerance and maturation time (Nagai et al., 2002). Criteria to consider when selecting donor and acceptor fluorescent moieties is known in the art, for instance as disclosed in U.S. Pat. No 6,197, 928, which is herein incorporated by reference in its entirety. An alternative is the use of a single fluorescent moiety such

as circularly-permuted variations of GFP (Akerboom et al., 2008) inserted into the backbone of LldR or other suitable lactate-binding protein, which undergoes a change in fluorescence intensity in response to binding of lactate to the LldR moiety or to other suitable lactate-binding protein. A variant of yellow fluorescent protein with fast and efficient maturation for cell-biological applications. Nagai T, Ibata K, Park ES, Kubota M, Mikoshiba K, Miyawaki A. Nat Biotechnol. 2002 Jan;20(1):87-90. Crystal structures of the GCaMP calcium sensor reveal the mechanism of fluorescence signal change and aid rational design. Akerboom J, Rivera JD, Guilbe MM, Malavé EC, Hernandez HH, Tian L, Hires SA, Marvin JS, Looger LL, Schreiter ER. J Biol Chem. 2009 Mar 6;284(10):6455-64. Epub 2008 Dec 18.

In a more preferred embodiment, the FRET pair selected was mTFP and Venus, which compared with CFP and YFP are respectively brighter and less pH-sensitive.

The general architecture search for structural combinations of the sensors is shown in Fig. 1a, with mTFP located at the N-terminus, the LldR flanked by linkers, and Venus located at the C-terminus.

Three constructs were generated for each bacterial species, differing with respect to the presence of DNA binding domain and linkers (Fig. 3). A comparative analysis showed that three proteins that changed their fluorescence in response to lactate, showed that constructs with LldR from *E. coli* changed their fluorescence ratio much more than those from *C. glutamicum*. The list of sequences comprises different embodiments of the invention, which should not be considered as limiting of the invention.

In a further embodiment, the present invention includes lactate nanosensors described according to the amino acid sequences and have at least 60%, 70%, 80% 85%, 90%, 95%, or 99% sequence identity with SEQ ID NO 1, SEQ ID NO 2, SEQ ID NO 3, SEQ ID NO 4, SEQ ID NO 5, SEQ ID NO 6, SEQ ID NO 7, SEQ ID NO 8, SEQ ID NO 9, SEQ ID NO 10, SEQ ID NO 11, SEQ ID NO 12, SEQ ID NO 13, SEQ ID NO 14, SEQ ID NO 15, or SEQ ID NO 16.

The present invention also considers the nucleic acid sequences having at least 60%, 70%, 80% 85%, 90%, 95%, or 99% sequence identity with SEQ ID NO 17, SEQ ID NO 18, SEQ ID NO 19, SEQ ID NO 20, SEQ ID NO 21, SEQ ID NO 22, SEQ ID NO 23, SEQ ID NO 24, SEQ ID NO 25, SEQ ID NO 26, SEQ ID NO

27, SEQ ID NO 28, SEQ ID NO 29, SEQ ID NO 30, SEQ ID NO 31, or SEQ ID NO 32.

The sequences described in SEQ ID NO 1 to SEQ ID NO 16 are only particular embodiments of the present invention provided as way of exemplification of the present invention, and should not be considered to limit the scope of the invention.

Also surprising was the observation that the DNA-binding domain is important for the FRET change, and that the sensors with no linkers are more responsive (Fig. 4). The most responsive variant, arrowed in Fig. 4, was chosen for further characterization. It contains the full length LldR from *E. coli* and no linkers. The emission spectrum of this nanosensor showed the expected peaks of mTFP and Venus at 492 nm and 526 nm, respectively (Fig. 5). The affinity constant of LldR for L-lactate is not known. Figure 6 shows that this nanosensor responded to a wide range of the ratio between mTFP and Venus. Fluorescence (at 430 nm excitation) was measured at increasing lactate concentrations, behavior well represented by a double rectangular hyperbola, with apparent dissociation constant (KD) values of 8 ± 2 μM and 830 ± 160 μM, and respective maximum ΔR values of 8 ± 0.4 % and 11 ± 0.4 %. This unique property of LldR confers the lactate sensor the desirable ability of reporting across four orders of magnitude (from 1 μM to 10 mM), instead of the two orders afforded by one-site sensors.

When used in vitro, the sensitivity of this nanosensor is similar to at least the most sensitive enzyme-based commercially available kit (50 pmoles).

The specificity was investigated by exposing the sensor to millimolar levels of several organic acids and glucose, of which only lactate induced a significant change in FRET (Fig. 7). The sensor showed a modest sensitivity to pH in the physiological range (Fig. 8). Expressed in mammalian cells, the lactate sensor of the present invention distributed in the cytosol and was excluded from nuclei and organelles (Fig. 9). Compared to the glucose sensor, its distribution was more heterogeneous, possibly due to LldR multimerization, but this did not affect the response to lactate (Supplementary Fig. 10). Expressed in cells, the sensor showed emission spectra and two-component dose-response curve similar to that observed in vitro, but with a larger change in FRET ratio (Fig. 11). In order to express fluorescence data in terms of lactate concentration, a single-point calibration

protocol is applied at the end of each experiment. Briefly, intracellular lactate is first lowered by depriving the cells of lactate and glucose, a maneuver that decreases the glycolytic flux and lowers the cytosolic NADH:NAD+ ratio (Hung et al., 2011; Zhao et al., 2011), inhibiting lactate production at Lactate dehydrogenase (LDH). To ensure that cytosolic lactate is indeed negligible, we use a property of MCTs termed trans-acceleration or accelerated exchange (Halestrap and Price, 1999). Cells are exposed to pyruvate, which on entering via MCT, increases in the number of inward-facing binding sites available for lactate extrusion, effectively "pumping out" the residual lactate. With the value for the fluorescence ratio at this "zero" lactate condition, the kinetic constants determined in vitro, and the maximum change of fluorescence ratio of 38% or the value determined in the specific cell type, fluorescence data were converted into lactate concentration as shown in Fig. 12. After 20 minutes of glucose/lactate deprivation in HEK293 cells or neurons, or 1 hour deprivation in astrocytes, intracellular lactate is undetectable (data not shown), consistent with the very low NADH:NAD+ ratio present under such conditions (Hung et al., 2011; Zhao et al., 2011).

The invention further comprises methods using the aforementioned nanosensor for determination of lactate concentrations in single cells or cell populations, adherent cells or in suspension, in a cell culture, a tissue culture, a mixed cell culture, a tissue explant, or in animal tissues *in vivo*.

The method comprises the general steps of:

a) Expressing the nanosensor of the invention, in a desired host, such as single cells or cell populations, adherent cells or in suspension, in a cell culture, a tissue culture, a mixed cell culture, a tissue explant, or in animal tissues *in vivo*;

b) Calibrating the host with predetermined values of intracellular, extracellular, subcellular lactate concentrations, recording lactate concentrations in time;

c) Disrupting the steady-state of lactate entering the cell;

d) Recording the output from the nanosensor calculating the lactate concentration at different time points;

In the step b), corresponding to calibrating the host, the nanosensor of the invention is calibrated in cells using the kinetic constants of the sensor obtained *in vitro* and a

zero-lactate level determined in the presence of pyruvate. Pyruvate can be in the range of 5 mM to 20mM, preferentially 10 mM.

The general method can be applied in different configurations, for example, in a first embodiment, the nanosensor is used in a method for the measurement of the activity of the lactate transporter.

In this first embodiment, with the information obtained in the calibration step, the disruption of the steady-state of lactate entering the cell is carried out by altering the extracellular concentration of lactate, thus exposing the cells to lactate. This causes a rise in intracellular lactate that is monitored with the lactate sensor and whose initial rate is independent of lactate metabolism and can be used to estimate kinetic parameters. Exposure of the cells to increasing concentrations of lactate allows the estimation of kinetic parameters for the lactate transporter. Kinetic parameters are also obtained from the decrease in intracellular lactate after removal of extracellular lactate.

In a second embodiment, the general method can be applied to a method to measure the rates of lactate production and lactate consumption.
In this second embodiment, with the information obtained in the calibration step, the steady-state of lactate is disrupted by altering the function of lactate transporter, for example by addition of a blocker of the lactate transporter. In mammalian cells, the lactate transporter is the MCT and can be blocked with phloretin, parachloromercurybenzoate or other suitable compounds. If the cell is a net lactate producer, application of the MCT-blocker causes an increase in intracellular lactate concentration, the initial rate of which is equal to the rate of cellular lactate production in the steady-state. If the cell is a net lactate importer, application of the MCT-blocker causes a fall in intracellular lactate concentration, the initial rate of which is equal to the rate of lactate consumption on the steady-state. In a more particular embodiment, the disruption of the steady-state is attained by adding an inhibitor of the MCT, such as, but not limited to phloretin, parachloromercurybenzoate, anti-MCT antisera, etc. In cells where lactate transport is mediated by other transporters, the method can be applied using their respective inhibitors. A critical property of this nanosensor that allows quantitation of these rates is its high temporal resolution, for only the initial rate of lactate accumulation is informative and after a few seconds other non-linear processes like inhibition of

glycolysis by the increasing lactate or changes in mitochondrial pyruvate uptake may interfere with the measurement. Because of its low temporal resolution, extracellular lactate measurement by existing techniques cannot be used in combination with MCT-blockage to estimate the rates of lactate production or lactate consumption.

In a third embodiment, the general method can be applied to a method to measure the rate of mitochondrial pyruvate consumption.

In this third embodiment, with the information obtained in the calibration step, the disruption in the lactate steady-state is caused by disrupting the flux of lactate. To quantitate the rate of mitochondrial pyruvate consumption, the steady-state is disrupted by addition of a blocker of the mitochondrial pyruvate transporter. In mammalian cells, the mitochondrial pyruvate transporter can be blocked with low concentration of 4-CIN. In cells, the concentration of pyruvate and lactate move together as a single pool because of fast interconversion by the high activity enzyme lactate dehydrogenase (LDH), with lactate representing over 90% of the pool. Application of the pyruvate transporter-blocker 4-CIN or other suitable inhibitor of the mitochondrial pyruvate transporter, causes an increase in the intracellular lactate concentration, the initial rate of which is equal to the rate of pyruvate uptake in the steady-state. In cells were pyruvate uptake into mitochondria were mediated by other transporters, the method could be applied using their respective inhibitors. A critical property of this nanosensor that allows quantitation of these rates is its high temporal resolution, for only the initial rate of lactate accumulation is informative and after a few seconds other non-linear processes MCT-transport and inhibition of glycolysis by increasing lactate may interfere with the measurement. In the steady-state and in the presence of glucose and lactate as exclusive oxidative substrates, the rate of pyruvate consumption by mitochondria is equal to the rate of the tricarboxylic acid (TCA) cycle and equal to rate of oxidative phosphorylation (OXPHOS).

A fourth particular embodiment of the method of the present invention is determination of cancer staging by estimation of the ratio between lactate production and the rate of the TCA cycle in a sample. Cancer cells are less oxidative than normal cells, a phenomenon known as the Warburg effect, which is receiving renewed attention regarding cancer pathogenesis, diagnosis and possibly treatment.

Robust flux through glycolysis and pentose phosphate pathways in these cells are thought to provide building blocks for proliferation and a high redox tone, while the lactic acid exported acidifies the environment and facilitates tumor migration and metastasis. A plot of lactate production versus TCA cycle rate shows that T98G glioma cells can be distinguished from normal astrocytes (Fig. 3a-b), but a more sensitive parameter is the ratio between lactate production and the rate of the TCA cycle, which we have termed Warburg Index (Fig. 3c). In an alternative embodiment, the Warburg Index is estimated by calculating the ratio between lactate production (with phloretin or other MCT blocker) and the rate of intracellular lactate increase in response to inhibition of oxidative phosphorylation with azide or other suitable compound (Fig. 17), which is a parameter of how oxidative is the cell. This alternative version of the Warburg index gives a different value but is also very sensitive to the mitochondrial defects that characterize cancer cells, senescent cells and other conditions that produce the Warburg phenomenon.

These tools allow the functional study of cancer metabolism with single-cell resolution and are also readily adaptable to multi-well format for high-throughput analysis of metabolism in cancer and other diseases. The development of a sensor based on LldR provides the basis for creating a wide variety of novel indicators because the GntR superfamily, of which LldR is a member, has 270 other transcription factors that bind pyruvate, fatty acids, amino acids, TCA cycle intermediates, etc., which are possible candidates to serve as templates for genetically-encoded nanosensors.

Based on the lactate nanosensor of this invention, methods are presented that allow for the first time single-cell real-time quantification of the rates of lactate production and of the tricarboxylic acid (TCA) cycle. Both methods follow cytosolic accumulation of lactate immediately after blockage of selected transporters, in analogous fashion to the measurement of the rate of glucose consumption with a glucose sensor. In the steady-state, the intracellular concentration of lactate is kept constant by a dynamic balance between glycolytic production and lactate efflux (Fig. 2c). Perturbation of the steady-state by addition of an MCT blocker like phloretin is expected to cause intracellular lactate accumulation at a rate equal to the rate of lactate production. For net lactate importers, like liver cells and possibly neurons, the MCT blocker should decrease intracellular lactate at a rate equal to the

rate of lactate consumption. A similar rationale can be applied to the quantification of pyruvate consumption by mitochondria. The high activity of lactate dehydrogenase (LDH) in mammalian cells, couples the concentrations of lactate and pyruvate, which for this purposes can be considered as a single pool, with lactate representing > 90%. Acute inhibition of the mitochondrial pyruvate transporter (PT) with a low concentration of α-Cyano-4-hydroxycinnamate (4-CIN) should produce an accumulation of intracellular lactate, at the rate of pyruvate consumption, which in the absence of alternative mitochondrial substrates is equivalent to the rates of the TCA cycle and oxidative phosphorylation. Experimental demonstration of these methods is provided in Fig. 2d. On average, astrocytes presented a lactate production rate of 2 μM/s and a TCA cycle rate of 7.6 μM/s, consistent with their rate of glucose consumption of 2 - 6 μM/s[11]. Typical of cell lines, HEK293 cells were more glycolytic and less oxidative than astrocytes, with respective rates of lactate production and TCA cycle of 5.4 and 2.1 μM/s. Inhibition of mitochondrial ATP production with sodium azide caused a 26 ± 4 fold increase in the rate of lactate production, fitting the deviation of all pyruvate flux towards lactate production and the 3 - 4 fold increase observed in glucose consumption (Fig. 2e). Fitting a mathematical model to actual lactate measurements indicated that the initial slopes of the changes in lactate concentration triggered by the transport blockers underestimate the actual rates of lactate production and TCA cycle by less than 10% (Supplementary Fig. 7).

The following examples are provided to help in the understanding of the present invention, and should not be considered a limitation to the scope of the invention.

EXAMPLES

In order to help understanding the invention, the present invention will be explained with reference to specific examples:

Protein Purification. Plasmid constructs were transformed into E. coli BL21 (DE3). A single colony was inoculated in 100 ml of LB medium with 100 mg/ml ampicillin (without IPTG) and shaken in the dark for 2-3 days. Cells were collected by centrifugation at 5000 rpm (4°C) for 10 min and disrupted by sonication (Hielscher Ultrasound Technology) in 5 mL of Tris-HCl buffer pH 8.0. A cell-free

extract was obtained by centrifugation at 10,000 rpm (4°C) for 1 hour and filtering of the supernatant (0.45 μm). Proteins were purified using a Nickel resin (His Bin® from Novagen) as recommended by the manufacturer. Eluted proteins were quantified using the Biuret method and stored at -20°C in 20% glycerol. The variant that showed the largest change in fluorescence ratio, was cloned into pcDNA3.1(-) for expression in eukaryotic cells using the restriction sites BamHI and HindIII.

Animals and Cell Cultures. Animals used were mixed F1 male mice (C57BL/6J x CBA/J), kept in an animal room under Specific Pathogen Free (SPF) conditions at a room temperature of 20 ± 2°C, in a 12/12 h light/dark cycle with free access to food and water. Experiments were approved by the Centro de Estudios Científicos Animal Care and Use Committee. Mixed cortical cultures of neuronal and glial cells (1-3 day-old neonates) were prepared as described (Loaiza et al., 2003). HEK293 and T98G glioma cells were acquired from the American Tissue Culture Collection and cultured at 37°C in 95% air/5% CO_2 in DMEM/F12 10% fetal bovine serum. Cultures were transfected at 60% confluence using Lipofectamine 2000 (Gibco) or alternatively, exposed to 5 x 10^6 PFU of Ad lactate sensor of the present invention (Vector Biolab), and studied after 24-72 h.

Fluorescence Measurements. Nickel-purified proteins were resuspended at 100 nM in an intracellular buffer containing (mM): 10 NaCl, 130 KCl, 1.25 MgSO4 and 10 HEPES, pH 7.0, and measured with a microplate reader analyzer (EnVision, PerkinElmer). The proteins were excited at 430 nm and the intensity of fluorescence emission of mTFP and Venus were recorded at 485 nm (FmTFP) and 528 nm (FVenus), respectively. The ratio (R) between FmTFP and FVenus was used to characterize the sensors. Emission spectra were obtained at 430 nm excitation, with 2 nm windows. Cells were imaged at room temperature (22 - 25°C) in a 95% air/5% CO_2-gassed solution of the following composition (in mM): 112 NaCl, 1.25 $CaCl_2$, 1.25 $MgSO_4$, 1-2 glucose, 10 HEPES, 24 $NaHCO^3$, pH 7.4, with 3 mM KCl (astrocytes) or 5 mM KCl (HEK and T98G) using an upright Olympus FV1000 Confocal Microscope equipped with a 20x water immersion objective (N.A. 1.0) and a 440 nm solid-state laser. Alternatively, cells were imaged with an Olympus IX70 or with an Olympus BX51 microscope equipped with a 40x oil-immersion objective (NA 1.3) or with a 20x water-immersion objective (NA 0.95). Microscopes were equipped with CAIRN monochromators (Faversham, UK), and either a Hamamatsu

Orca camera controlled by Kinetics software or a Rollera camera controlled with Metafluor software, respectively. For nanosensor ratio measurements, cells were excited at 430 nm for 0.2-0.8 s. Emission was divided with a CAIRN Optosplit, equipped with band pass filters at 480 ± 20 (FmTFP) and 535 ± 15 nm (FVenus). The ratio between FmTFP and FVenus was used to measure lactate. The pH-sensitive dye BCECF was ester loaded at 0.1 μM for 3-4 min and the signal was calibrated by exposing the cultures to solutions of different pH after permeabilizing the cells with 10 μg/ml nigericin and 20 μg/ml gramicidin in an intracellular buffer. BCECF was sequentially excited at 440 and 490 nm (0.05 s) and imaged at 535 ± 15 nm.

Mathematical Modeling of Lactate Dynamics. A model of intracellular lactate dynamics was generated according to the flux diagram in Fig. 14 and 16, in the absence of extracellular lactate,

$$d[Pyr]/dt = (G + [Lac]*LDHr - [Pyr]*LDHf - PT)/vol$$
$$d[Lac]/dt = ([Pyr]*LDHf - [Lac]*LDHr - VMCT/\{KMCT+[Lac]\})/vol$$

where [Pyr] is cytosolic pyruvate concentration, [Lac] is cytosolic lactate concentration, G is glycolytic pyruvate production, LDHf and LDHr are the lactate dehydrogenase forward and reverse reactions and PT is mitochondrial pyruvate uptake. MCT efflux obeys Michaelis-Menten kinetics with maximum rate VMCT and an apparent affinity KMCT (5 mM). The kinetic model was solved numerically with the computer software Berkeley Madonna using the Rosenbrock method.

Statistical Analysis. All time courses correspond to single cells. Experiments were repeated three to six times, with 6-12 cells per experiment. Regression analyses were carried out with the computer program SigmaPlot (Jandel). Differences in mean values of paired samples were evaluated with the Student's t-test. P values < 0.05 were considered significant and are indicated with an asterisk (*).

Sixteen different variants of the lactate nanosensor, according to different embodiments of the present invention were produced. Figure 4 shows the response to lactate of the sixteen variants of the lactate sensor, wherein the black filled bars correspond to the variants 1, 3, 5, 7, 9, 11, 13, 15, and the grey filled bars correspond to variants 2, 4, 6, 8, 10, 12, 14, and 16. Each of the produced variants of

the lactate nanosensor of the present invention are encoded by the aminoacid sequence described in the list, SEQ ID NO 1 corresponding to variant 1, SEQ ID NO 2 corresponding to variant 2, SEQ ID NO 3 corresponding to variant 3, SEQ ID NO 4 corresponding to variant 4, SEQ ID NO 5 corresponding to variant 5, SEQ ID NO 6 corresponding to variant 6, SEQ ID NO 7 corresponding to variant 7, SEQ ID NO 8 corresponding to variant 8, SEQ ID NO 9 corresponding to variant 9, SEQ ID NO 10 corresponding to variant 10, SEQ ID NO 11 corresponding to variant 11, SEQ ID NO 12 corresponding to variant 12, SEQ ID NO 13 corresponding to variant 13, SEQ ID NO 14 corresponding to variant 14, SEQ ID NO 15 corresponding to variant 15, SEQ ID NO 16 corresponding to variant 16. Most of the variants showed a measureable change in fluorescence ratio in response to lactate and may be used for the different methods described in the present invention. The high rate of successful sensor generation shows a surprising robustness of LldR as a scaffold for FRET-based sensor generation.

Example 1. Method for the measurement of lactate transporter activity with high spatiotemporal resolution.

By controlling the exchange of lactate between cells and the interstitial space, MCTs are nodal points of tissue metabolism. MCTs catalyze the stoichiometric translocation of lactate and a proton and their activity can be measured with single-cell resolution by monitoring intracellular pH with a dye such as BCECF. However, 99.9% of protons are bound to proteins, phospholipids and other sites, and are exchanged through many transporters other than the MCT, which makes pH an imperfect proxy for lactate. To compare the performances of the lactate sensor of the present invention and BCECF, we chose astrocytes. When expressed in astrocytes, the lactate sensor of the present invention responded well to extracellular lactate, allowing real-time monitoring of lactate influx and efflux (Fig. 13). Consistent with an MCT-mediated process, the initial rate of astrocytic uptake of 1 mM lactate of 1.6 ± 0.5 μM/s was inhibited by 96 ± 1 % in the presence of the MCT blocker phloretin (50 μM). In contrast, exposure to extracellular lactate produced only a small change in intracellular pH as detected with BCECF (Fig. 15). Thus, the lactate sensor can be used to measure MCT, allowing a more sensitive and physiological characterization of their function. Lactate may also be transported

independently of protons through gap junctions (Rouach et al., 2008) and possibly through connexin hemichannels and pannexin channels, fluxes that are invisible to pH measurements and that may now be measured with the present invention.

Example 2. Metabolic rate of pyruvate consumption by mitochondria.

The diagram in Fig. 14 illustrates how the intracellular concentration of lactate is determined by the dynamic balance between pyruvate production by glycolysis, pyruvate consumption by mitochondria and lactate exchange through MCTs. In cells that are exporting lactate, perturbation of the steady state by addition of a blocker of the MCT is expected to cause lactate accumulation. In cells that are net lactate importers, an MCT-blocker is expected to cause depletion in intracellular lactate. In both cases, the rate of change will be equal to the rate of lactate production or consumption. As a demonstration of the principle in HEK293 cells and in astrocytes, MCT inhibition with phloretin (50 μM) caused the expected increase in intracellular lactate, indicative of lactate production (Fig. 15). Phloretin is also known to inhibit GLUT glucose transporters, however this should not compromise the analysis of astrocytes, neurons, or the cell lines so far characterized, which maintain resting intracellular glucose at levels well above the Km of hexokinase (Bittner et al., 2010; Takanaga et al., 2008; Fehr et al., 2003). In these cells, glucose consumption remains constant for several minutes in the presence of glucose transporter blockers like phloretin or cytochalasin B (Bittner et al., 2010). Thus, during the first few minutes of phloretin application, the rate of lactate accumulation is not diminished by lack of glucose supply. In muscle cells and adipocytes, which maintain low levels of intracellular glucose, a more selective MCT inhibitor may be used (Ovens et al., 2010).

Example 3. Method to measure the rate of mitochondrial metabolism with high spatiotemporal resolution.

Because the reaction catalyzed by LDH is relatively fast, the cytosolic pools of lactate and pyruvate are tightly linked, and variations in pyruvate are faithfully mimicked by lactate. Accordingly, perturbation of the steady-state by addition of a blocker of the mitochondrial pyruvate transporter (PT) will cause intracellular lactate accumulation at a rate equal to the rate of pyruvate consumption by

mitochondria. As predicted by the kinetic model, inhibition of the mitochondrial pyruvate transporter in HEK293 cells with α-cyano-4-hydroxycinnamate (4-CIN) at a concentration that does not affect MCT function (Halestrap and Denton, 1975), led to an increase in intracellular lactate (Fig. 15). As typical of cell lines, HEK293 cells were more glycolytic than oxidative, having respective rates of lactate production and pyruvate uptake of 5.4 and 2.1 μM/s, whereas on average, astrocytes demonstrated a lactate production of 2 μM/s and pyruvate uptake of 7.6 μM/s (Fig. 15), consistent with their rate of glucose consumption of 2 - 6 μM/s (Bittner et al., 2010; Bittner et al., 2011).

To further validate methods 2 and 3, the blockers were applied sequentially and a mathematical model based on the kinetic model described in Fig. 14 was fitted to the data. The responses of intracellular lactate to transient inhibitions of the PT with 4-CIN (200 μM) and the MCTs with phloretin (50 μM) were measured in the same HEK293 cell in the presence of 25 mM glucose and no extracellular lactate. The straight lines represent the slopes of the lactate increases fitted by linear regression during the first minute (4-CIN) or during the whole exposure (phloretin). The red line represents the best fit of the kinetic model to the data, as described in Experimental Procedures, assuming full inhibition of the transporters. Fitted parameters were: G = 10.3 μM/s, PT = 4.8 μM/s, LDHf = 9 s-1, LDHr = 0.45 s-1, Vmax= 186 μM/s, G-PT (lactate production)= 5.5 μM/s. PT and lactate release rates respectively estimated from the initial slopes of lactate increase after transporter inhibition were over 90% of those estimated by modeling. As shown in Fig. 16, the rate of lactate accumulation induced by 4-CIN was maximal at the onset of inhibition and then declined, due to increased efflux through the MCT as lactate accumulated. Therefore, only the initial rate of lactate accumulation will represent mitochondrial metabolism accurately. In contrast, MCT blockage resulted in sustained accumulation of lactate, a finding that is consistent with the accepted notions that glycolytic pyruvate production and mitochondrial pyruvate consumption are not modulated by cytosolic pyruvate. On the other hand, the limited accumulation of lactate caused by 4-CIN confirms that 4-CIN did not block MCTs to a significant extent. The best fit of the model to the data showed that the initial slopes of the changes in lactate concentration triggered by the transport blockers

underestimate the actual rates of mitochondrial pyruvate uptake and lactate production by less than 10%.

Example 4. Detection of drugs that interfere with mitochondrial metabolism with high spatiotemporal resolution.

The screening for unwanted effects is an important part of the process of drug discovery. One possibility to be ruled out before the drug is tested in animals or humans is the possibility that a candidate drug may exert undesirable effects on cellular energy metabolism. An inhibition of mitochondrial ATP production is compensated by increase in glycolytic ATP production and lactate production. Typically, a 3-4 fold increase in the rate of glucose consumption is observed (Bittner et al., 2010). However, the increase in lactate production can be much higher, because without the mitochondrial pyruvate sink, all glucose is now converted into lactate. Taking advantage of the improved resolution of the lactate sensor of the present invention, a method is presented that detects mitochondrial poisoning with very high sensitivity. As an example of this method, an acute inhibition of oxidative phosphorylation in astrocytes with 5 mM azide caused a 26 ± 4 -fold increase in the rate of lactate production measured with the lactate sensor of the present invention (Fig 17a). Fig. 17b shows the acute effect of azide 5 mM on the intracellular concentration of lactate. Used in multi-well plate format, both protocols may be incorporated in high throughput applications for the screening of mitochondrial interference.

Example 5. Detection of the Warburg effect in single cells with high temporal resolution.

Augmented flux through glycolysis and the pentose phosphate pathway in cancer cells provides the building blocks for proliferation and a high redox state that protects them against free radicals released during chemotherapy, while the lactic acid exported via MCTs acidifies the tumor environment and facilitates cell migration and metastasis. The glycolytic nature of cancer cells even in the presence of oxygen, a phenomenon known as the Warburg effect, is detected by comparing lactate production with oxygen consumption, measurements that demand large numbers of cells and overlook tissue heterogeneity. The reversible nature of

mitochondrial flux and lactate production measurements with the lactate sensor allowed a more refined characterization of the Warburg phenotype. A comparison of astrocytes with T98G glioblastoma cells, showed that the non-transformed cells are more oxidative than their tumor counterparts (Figs. 18 and 19). The difference between normal and cancerous cells was dramatically amplified by lactate production and pyruvate uptake, to give a parameter of cell metabolism that we have termed Warburg Index (WI). Some glioblastoma cells behaved almost like an astrocyte but some presented Warburg Index values that were 100 times higher than that of a normal astrocyte (Fig. 20). Tumors are known to be metabolically heterogeneous, which is expected given unequal access of their cells to oxygen and nutrients, but it seems remarkable that a cell line like T98G, cultured under carefully controlled conditions at high oxygen levels be also so heterogeneous from the metabolic point of view. The single-cell real-time capability of the lactate sensor should allow a metabolic characterization of individual cells and cell lineages in tumors and tissue explants. Used in cell populations with a multi-well plate reader, it is readily amenable for high throughput applications. An alternative embodiment of Example 5 replaces 4-CIN with an inhibitor of oxidative phosphorylation like azide or rotenone.

While certain embodiments of the invention have been described, other embodiments may exist. Further, any disclosed method steps or stages may be modified in any manner, including by reordering steps and/or inserting or deleting steps, without departing from the invention. While the specification includes a detailed description of the nanosensor and the associated drawings, the invention's scope is indicated by the following claims. Furthermore, while the specification has been described in a specific language, the claims are not limited to the features or acts described above. Rather, the specific features and acts described above are disclosed as illustrative aspects and embodiments of the invention. Various other aspects, embodiments, modifications, and equivalents thereof which, after reading the description herein, may suggest themselves to one of ordinary skill in the art without departing from the spirit of the present invention or the scope of the claimed subject matter.

LIST OF REFERENCES

- Brooks,G.A. J. Physiol 587, 5591-5600 (2009).
- Barros,L.F. & Deitmer,J.W. Brain Res. Rev. 63, 149-159 (2010).
- Ganapathy,V., Thangaraju,M., & Prasad,P.D. Pharmacol. Ther. 121, 29-40 (2009).
- Vander Heiden,M.G., Cantley,L.C., & Thompson,C.B. Science. 324, 1029-1033 (2009).
- Pellerin,L. et al. Glia. 55, 1251-1262 (2007).
- Gao,Y.G. et al. Nucleic Acids Res. 36, 7110-7123 (2008).
- Aguilera,L. et al. J. Bacteriol. 190, 2997-3005 (2008).
- Deuschle,K. et al. Protein Sci. 14, 2304-2314 (2005).
- Day,R.N., Booker,C.F., & Periasamy,A. J. Biomed. Opt. 13, 031203 (2008).
- Nagai,T. et al. Nat. Biotechnol. 20, 87-90 (2002).
- Bittner,C.X. et al. Front. Neuroenergetics 2, 1-11 doi: 10.3389/fnene.2010.00026 (2010).
- Ovens,M.J. et al. Biochem. J. 425, 523-530 (2010).
- Becker,H.M., Broer,S., & Deitmer,J.W. Biophys. J. 86, 235-247 (2004).
- Halestrap,A.P. & Denton,R.M. Biochem. J. 148, 97-106 (1975).
- Georgi,T., Engels,V., & Wendisch,V.F. J. Bacteriol. 190, 963-971 (2008).
- Nagai T, Ibata K, Park ES, Kubota M, Mikoshiba K, Miyawaki A. Nat Biotechnol. 2002 Jan;20(1):87-90.
- Akerboom J, Rivera JD, Guilbe MM, Malavé EC, Hernandez HH, Tian L, Hires SA, Marvin JS, Looger LL, Schreiter ER. J Biol Chem. 2009 Mar 6;284(10):6455-64. Epub 2008 Dec 18.

CLAIMS

What is claimed is:

1. A Forster Resonance Energy Transfer (FRET)-based lactate nanosensor comprising a bacterial LldR transcription factor between any suitable donor and acceptor fluorescent proteins moieties that are capable in combination of serving as donor and acceptor moieties in FRET, which can be expressed in single cells or cell populations, adherent cells or in suspension, in a cell culture, a tissue culture, a mixed cell culture, a tissue explant, or in animal tissues in vivo.

2. A FRET-based lactate nanosensor according to claim 1, wherein the fluorescent proteins moieties are selected among from the group consisting of mTFP (monomeric teal fluorescent protein), CFP (cyan fluorescent protein), BFP (blue fluorescent protein), GFP (green fluorescent protein), YFP (yellow fluorescent protein), enhanced variations thereof such as enhanced YFP (EYFP), YFP-Citrine, Venus, or infrared fluorescent proteins from bacterial phytochromes.

3. FRET-based lactate nanosensor according to claim 1, wherein the fluorescent proteins moieties are mTFP and Venus.

4. A FRET-based lactate nanosensor according to claim 1 or 3, having at least 60%, 70%, 80% 85%, 90%, 95%, or 99% amino acid sequence identity with SEQ ID NO 1, SEQ ID NO 2, SEQ ID NO 3, SEQ ID NO 4, SEQ ID NO 5, SEQ ID NO 6, SEQ ID NO 7, SEQ ID NO 8, SEQ ID NO 9, SEQ ID NO 10, SEQ ID NO 11, SEQ ID NO 12, SEQ ID NO 13, SEQ ID NO 14, SEQ ID NO 15, or SEQ ID NO 16.

5. FRET-based lactate nanosensor according to claim 1 or 3, encoded by the nucleic acid sequences having at least 60%, 70%, 80% 85%, 90%, 95%, or 99% sequence identity with SEQ ID NO 17, SEQ ID NO 18, SEQ ID NO 19, SEQ ID NO 20, SEQ ID NO 21, SEQ ID NO 22, SEQ ID NO 23, SEQ ID

NO 24, SEQ ID NO 25, SEQ ID NO 26, SEQ ID NO 27, SEQ ID NO 28, SEQ ID NO 29, SEQ ID NO 30, SEQ ID NO 31, or SEQ ID NO 32.

6. A method for the measurement of lactate wherein the method comprises the steps of:
    a. Expressing a FRET-based lactate nanosensor in a desired host, such as single cells or cell populations, adherent cells or in suspension, in a cell culture, a tissue culture, a mixed cell culture, a tissue explant, or in animal tissues in vivo;
    b. Calibrating the host with predetermined values of intracellular, extracellular, subcellular lactate concentrations, recording lactate concentrations in time;
    c. Disrupting the steady-state of lactate in the cell;
    d. Recording the output from the nanosensor calculating the lactate concentration at different time points and determining the rates of transport.

7. Method for the measurement of lactate according to claim 6, wherein in step b) the FRET-based lactate nanosensor in cells is calibrated by using the kinetic constants of the sensor obtained *in vitro* and a zero-lactate level determined in the presence of pyruvate.

8. Method for the measurement of lactate according to claim 7, wherein in step c) the disruption of lactate steady-state is by exposing cells to varying concentrations of extracellular lactate.

9. A method for the measurement of the rate of lactate production or consumption wherein the method comprises the steps of:
    a. Expressing a FRET-based lactate nanosensor in a desired host, such as single cells or cell populations, adherent cells or in suspension, in a cell culture, a tissue culture, a mixed cell culture, a tissue explant, or in animal tissues in vivo;

b. Calibrating the host with predetermined values of intracellular, extracellular, subcellular lactate concentrations, recording lactate concentrations in time;
c. Disrupting the steady-state of lactate in the cell;
d. Recording the output from the nanosensor calculating the lactate concentration at different time points and determining the rates of transport.

10. Method for the measurement of the rate of lactate production or consumption according to claim 9, wherein in step b) the FRET-based lactate nanosensor in cells is calibrated by using the kinetic constants of the sensor obtained *in vitro* and a zero-lactate level determined in the presence of pyruvate.

11. Method for the measurement of the rate of lactate production or consumption according to claim 9, wherein in step c) the disruption of lactate steady-state is by adding an MCT inhibitor which measures the rates of lactate accumulation, equal to the rate of lactate production, or lactate depletion, equal to the rate of lactate consumption.

12. A method for the measurement of the rate of mitochondrial pyruvate consumption wherein the method comprises the steps of:
    a. Expressing a FRET-based lactate nanosensor in a desired host, such as single cells or cell populations, adherent cells or in suspension, in a cell culture, a tissue culture, a mixed cell culture, a tissue explant, or in animal tissues in vivo;
    b. Calibrating the host with predetermined values of intracellular, extracellular, subcellular lactate concentrations, recording lactate concentrations in time;
    c. Disrupting the steady-state of lactate in the cell;
    d. Recording the output from the nanosensor calculating the lactate concentration at different time points and determining the rates of transport.

13. Method for the measurement of the rate of the rate of mitochondrial pyruvate consumption according to claim 12, wherein in step b) the FRET-based lactate nanosensor in cells is calibrated by using the kinetic constants of the sensor obtained *in vitro* and a zero-lactate level determined in the presence of pyruvate.

14. Method for the measurement of the rate of mitochondrial pyruvate consumption according to claim 12, wherein in step c) the disruption of lactate steady-state is by adding a blocker of the mitochondrial pyruvate transporter and measures the initial rate of lactate accumulation, which is equal to the rate of pyruvate consumption by mitochondria.

15. A method for the quantification of the Warburg phenomenon wherein the method comprises the steps of:
    a. Expressing a FRET-based lactate nanosensor in a desired host, such as single cells or cell populations, adherent cells or in suspension, in a cell culture, a tissue culture, a mixed cell culture, a tissue explant, or in animal tissues in vivo;
    b. Calibrating the host with predetermined values of intracellular, extracellular, subcellular lactate concentrations, recording lactate concentrations in time;
    c. Disrupting the steady-state of lactate in the cell;
    d. Recording the output from the nanosensor calculating the lactate concentration at different time points and determining the rates of transport; and
    e. Quantifying the Warburg phenomenon by calculating the ratio between the rate of lactate accumulation in the presence of an MCT inhibitor, and the rate of lactate accumulation in the presence of an inhibitor of the mitochondrial pyruvate transporter.

16. Method for the quantification of the Warburg phenomenon consumption according to claim 15, wherein in step b) the FRET-based lactate nanosensor

in cells is calibrated by using the kinetic constants of the sensor obtained *in vitro* and a zero-lactate level determined in the presence of pyruvate.

17. Method for the quantification of the Warburg phenomenon according to claim 15, wherein in step c) the disruption of lactate steady-state is by adding an MCT inhibitor which measures the rates of lactate production or lactate consumption and adding a blocker of the mitochondrial pyruvate transporter, the method further including measuring the initial rate of lactate accumulation, which is equal to the rate of pyruvate consumption by mitochondria.

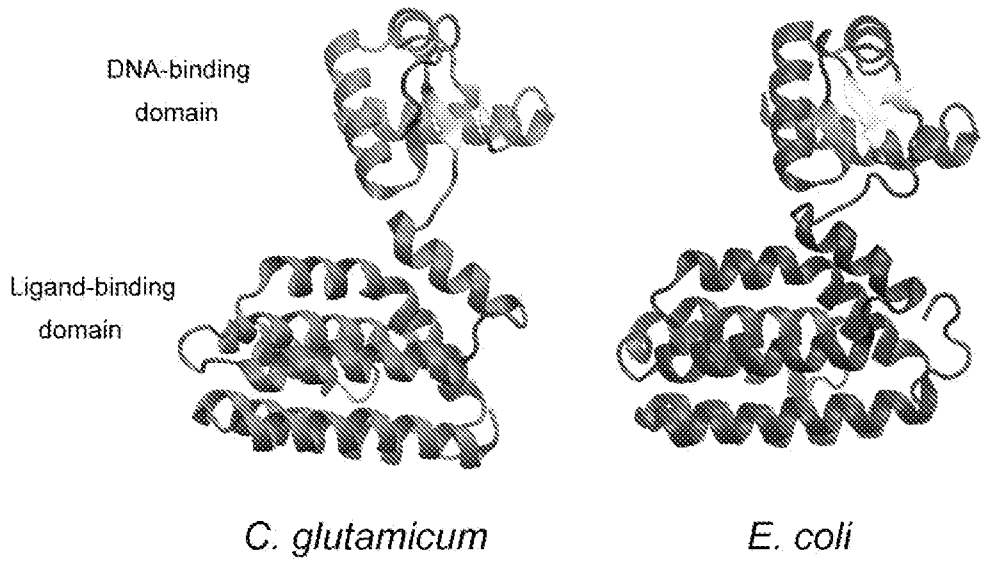
DNA-binding
domain
Ligand-binding
domain
C. glutamicum
E. coli

Figure 1

E. coli mivlpxxlsd evadrvxali dexnleagmx lpaexqlamq lgvsxnslxe
C. glutamicum msvxahesvm dwvteelxsg xlxigdhlps exalsetlgv sxsslxealx
1

E. coli alaxlvsegv llsxxgggtf ixwxhdtwse qnivqplxtl maddpdysfd
C. glutamicum vlealgtist atgsgpxsgt iitaapgqal slsvtlqlvt nqvghhdiye
51

E. coli ileaxyaiea stawhaamxa tpgdxexiql cfeatlsedp diasqadvxf
C. glutamicum txqllegwaa lhssaexgdw dvaeallexm ddpslpledf lxfdaefhvv
101

E. coli hlaiaeaashn ivllqtmxgf fdvlqssvxh sxqxmylvpp vfsqlteqhq
C. glutamicum isxgaenpli stlmealxls vadhtvaxax alpdwxatsa xlqxehxail
151

E. coli avidaifagd adgaxkamma hlsfvhttmx xfdedqaxha xitxlpgehn
C. glutamicum aalxagestv aatlikehie gyyeetaaae a
201

E. coli ehsxexna
C. glutamicum
251

FIGURE 2

FIGURE 3

Alignment of Lactate nanosensor variants

Section 1

```
            (1) 1        10        20        30        40                57
Variant 01  (1) MVSKGEETTMGVIKPDMKIKLKMEGNVNGHAFVIEGEGEGKPYDGTNTINLEVKEGA
Variant 02  (1) MVSKGEETTMGVIKPDMKIKLKMEGNVNGHAFVIEGEGEGKPYDGTNTINLEVKEGA
Variant 03  (1) MVSKGEETTMGVIKPDMKIKLKMEGNVNGHAFVIEGEGEGKPYDGTNTINLEVKEGA
Variant 04  (1) MVSKGEETTMGVIKPDMKIKLKMEGNVNGHAFVIEGEGEGKPYDGTNTINLEVKEGA
Variant 05  (1) MVSKGEETTMGVIKPDMKIKLKMEGNVNGHAFVIEGEGEGKPYDGTNTINLEVKEGA
Variant 06  (1) MVSKGEETTMGVIKPDMKIKLKMEGNVNGHAFVIEGEGEGKPYDGTNTINLEVKEGA
Variant 07  (1) MVSKGEETTMGVIKPDMKIKLKMEGNVNGHAFVIEGEGEGKPYDGTNTINLEVKEGA
Variant 08  (1) MVSKGEETTMGVIKPDMKIKLKMEGNVNGHAFVIEGEGEGKPYDGTNTINLEVKEGA
Variant 09  (1) MVSKGEETTMGVIKPDMKIKLKMEGNVNGHAFVIEGEGEGKPYDGTNTINLEVKEGA
Variant 10  (1) MVSKGEETTMGVIKPDMKIKLKMEGNVNGHAFVIEGEGEGKPYDGTNTINLEVKEGA
Variant 11  (1) MVSKGEETTMGVIKPDMKIKLKMEGNVNGHAFVIEGEGEGKPYDGTNTINLEVKEGA
Variant 12  (1) MVSKGEETTMGVIKPDMKIKLKMEGNVNGHAFVIEGEGEGKPYDGTNTINLEVKEGA
Variant 13  (1) MVSKGEETTMGVIKPDMKIKLKMEGNVNGHAFVIEGEGEGKPYDGTNTINLEVKEGA
Variant 14  (1) MVSKGEETTMGVIKPDMKIKLKMEGNVNGHAFVIEGEGEGKPYDGTNTINLEVKEGA
Variant 15  (1) MVSKGEETTMGVIKPDMKIKLKMEGNVNGHAFVIEGEGEGKPYDGTNTINLEVKEGA
Variant 16  (1) MVSKGEETTMGVIKPDMKIKLKMEGNVNGHAFVIEGEGEGKPYDGTNTINLEVKEGA
```

Section 2

```
            (58) 58          70        80        90        100          114
Variant 01  (58) PLPFSYDILTTAFAYGNRAFTKYPDDIPNYFKQSFPEGYSWERTMTFEDKGIVKVKS
Variant 02  (58) PLPFSYDILTTAFAYGNRAFTKYPDDIPNYFKQSFPEGYSWERTMTFEDKGIVKVKS
Variant 03  (58) PLPFSYDILTTAFAYGNRAFTKYPDDIPNYFKQSFPEGYSWERTMTFEDKGIVKVKS
Variant 04  (58) PLPFSYDILTTAFAYGNRAFTKYPDDIPNYFKQSFPEGYSWERTMTFEDKGIVKVKS
Variant 05  (58) PLPFSYDILTTAFAYGNRAFTKYPDDIPNYFKQSFPEGYSWERTMTFEDKGIVKVKS
Variant 06  (58) PLPFSYDILTTAFAYGNRAFTKYPDDIPNYFKQSFPEGYSWERTMTFEDKGIVKVKS
Variant 07  (58) PLPFSYDILTTAFAYGNRAFTKYPDDIPNYFKQSFPEGYSWERTMTFEDKGIVKVKS
Variant 08  (58) PLPFSYDILTTAFAYGNRAFTKYPDDIPNYFKQSFPEGYSWERTMTFEDKGIVKVKS
Variant 09  (58) PLPFSYDILTTAFAYGNRAFTKYPDDIPNYFKQSFPEGYSWERTMTFEDKGIVKVKS
Variant 10  (58) PLPFSYDILTTAFAYGNRAFTKYPDDIPNYFKQSFPEGYSWERTMTFEDKGIVKVKS
Variant 11  (58) PLPFSYDILTTAFAYGNRAFTKYPDDIPNYFKQSFPEGYSWERTMTFEDKGIVKVKS
Variant 12  (58) PLPFSYDILTTAFAYGNRAFTKYPDDIPNYFKQSFPEGYSWERTMTFEDKGIVKVKS
Variant 13  (58) PLPFSYDILTTAFAYGNRAFTKYPDDIPNYFKQSFPEGYSWERTMTFEDKGIVKVKS
Variant 14  (58) PLPFSYDILTTAFAYGNRAFTKYPDDIPNYFKQSFPEGYSWERTMTFEDKGIVKVKS
Variant 15  (58) PLPFSYDILTTAFAYGNRAFTKYPDDIPNYFKQSFPEGYSWERTMTFEDKGIVKVKS
Variant 16  (58) PLPFSYDILTTAFAYGNRAFTKYPDDIPNYFKQSFPEGYSWERTMTFEDKGIVKVKS
```

Section 3

```
            (115) 115  120       130       140       150       160       171
Variant 01  (115) DISMEEDSFIYEIHLKGENFPPNGPVMQKKTTGWDASTERMYVRDGVLKGDVKHKLL
Variant 02  (115) DISMEEDSFIYEIHLKGENFPPNGPVMQKKTTGWDASTERMYVRDGVLKGDVKHKLL
Variant 03  (115) DISMEEDSFIYEIHLKGENFPPNGPVMQKKTTGWDASTERMYVRDGVLKGDVKHKLL
Variant 04  (115) DISMEEDSFIYEIHLKGENFPPNGPVMQKKTTGWDASTERMYVRDGVLKGDVKHKLL
Variant 05  (115) DISMEEDSFIYEIHLKGENFPPNGPVMQKKTTGWDASTERMYVRDGVLKGDVKHKLL
Variant 06  (115) DISMEEDSFIYEIHLKGENFPPNGPVMQKKTTGWDASTERMYVRDGVLKGDVKHKLL
Variant 07  (115) DISMEEDSFIYEIHLKGENFPPNGPVMQKKTTGWDASTERMYVRDGVLKGDVKHKLL
Variant 08  (115) DISMEEDSFIYEIHLKGENFPPNGPVMQKKTTGWDASTERMYVRDGVLKGDVKHKLL
Variant 09  (115) DISMEEDSFIYEIHLKGENFPPNGPVMQKKTTGWDASTERMYVRDGVLKGDVKHKLL
Variant 10  (115) DISMEEDSFIYEIHLKGENFPPNGPVMQKKTTGWDASTERMYVRDGVLKGDVKHKLL
Variant 11  (115) DISMEEDSFIYEIHLKGENFPPNGPVMQKKTTGWDASTERMYVRDGVLKGDVKHKLL
Variant 12  (115) DISMEEDSFIYEIHLKGENFPPNGPVMQKKTTGWDASTERMYVRDGVLKGDVKHKLL
Variant 13  (115) DISMEEDSFIYEIHLKGENFPPNGPVMQKKTTGWDASTERMYVRDGVLKGDVKHKLL
Variant 14  (115) DISMEEDSFIYEIHLKGENFPPNGPVMQKKTTGWDASTERMYVRDGVLKGDVKHKLL
Variant 15  (115) DISMEEDSFIYEIHLKGENFPPNGPVMQKKTTGWDASTERMYVRDGVLKGDVKHKLL
Variant 16  (115) DISMEEDSFIYEIHLKGENFPPNGPVMQKKTTGWDASTERMYVRDGVLKGDVKHKLL
```

FIGURE 3 (Cont.)

```
Alignment of Lactate nanosensor variants
Section 4
            (172) 172     180       190       200       210             228
Variant 01  (172) LEGGGHHRVDFKTIYRAKKAVKLPDYHFVDHRIEILNHDKDYNKVTVYESAVARNST
Variant 02  (172) LEGGGHHRVDFKTIYRAKKAVKLPDYHFVDHRIEILNHDKDYNKVTVYESAVARNST
Variant 03  (172) LEGGGHHRVDFKTIYRAKKAVKLPDYHFVDHRIEILNHDKDYNKVTVYESAVARNST
Variant 04  (172) LEGGGHHRVDFKTIYRAKKAVKLPDYHFVDHRIEILNHDKDYNKVTVYESAVARNST
Variant 05  (172) LEGGGHHRVDFKTIYRAKKAVKLPDYHFVDHRIEILNHDKDYNKVTVYESAVARNST
Variant 06  (172) LEGGGHHRVDFKTIYRAKKAVKLPDYHFVDHRIEILNHDKDYNKVTVYESAVARNST
Variant 07  (172) LEGGGHHRVDFKTIYRAKKAVKLPDYHFVDHRIEILNHDKDYNKVTVYESAVARNST
Variant 08  (172) LEGGGHHRVDFKTIYRAKKAVKLPDYHFVDHRIEILNHDKDYNKVTVYESAVARNST
Variant 09  (172) LEGGGHHRVDFKTIYRAKKAVKLPDYHFVDHRIEILNHDKDYNKVTVYESAVARNST
Variant 10  (172) LEGGGHHRVDFKTIYRAKKAVKLPDYHFVDHRIEILNHDKDYNKVTVYESAVARNST
Variant 11  (172) LEGGGHHRVDFKTIYRAKKAVKLPDYHFVDHRIEILNHDKDYNKVTVYESAVARNST
Variant 12  (172) LEGGGHHRVDFKTIYRAKKAVKLPDYHFVDHRIEILNHDKDYNKVTVYESAVARNST
Variant 13  (172) LEGGGHHRVDFKTIYRAKKAVKLPDYHFVDHRIEILNHDKDYNKVTVYESAVARNST
Variant 14  (172) LEGGGHHRVDFKTIYRAKKAVKLPDYHFVDHRIEILNHDKDYNKVTVYESAVARNST
Variant 15  (172) LEGGGHHRVDFKTIYRAKKAVKLPDYHFVDHRIEILNHDKDYNKVTVYESAVARNST
Variant 16  (172) LEGGGHHRVDFKTIYRAKKAVKLPDYHFVDHRIEILNHDKDYNKVTVYESAVARNST

Section 5
            (229) 229       240       250       260       270             285
Variant 01  (229) DGMDELYKRSGTTSLYKKAGSEFALGTMIVLPRRLSDEVADRVRALIDEKNLEAGMK
Variant 02  (229) DGMDELYKRSGTTSLYKKAGSEFAL---GTMSVKAHESVMDWVTEELRSGRLKIGDH
Variant 03  (229) DGMDELYKRSGTM---------------IVLPRRLSDEVADRVRALIDEKNLEAGMK
Variant 04  (229) DGMDELYKRS-----------------GTMSVKAHESVMDWVTEELRSGRLKIGDH
Variant 05  (229) DGMDELYKRSGTTSLYKKAGSEFALGTMIVLPRRLSDEVADRVRALIDEKNLEAGMK
Variant 06  (229) DGMDELYKRSGTTSLYKKAGSEFAL---GTMSVKAHESVMDWVTEELRSGRLKIGDH
Variant 07  (229) DGMDELYKRSGTM---------------IVLPRRLSDEVADRVRALIDEKNLEAGMK
Variant 08  (229) DGMDELYKRS-----------------GTMSVKAHESVMDWVTEELRSGRLKIGDH
Variant 09  (229) DGMDELYKRSGTT---------------SLYKKAGSEFAL-----------------
Variant 10  (229) DGMDELYKRS-----------------G-----------------------------
Variant 11  (229) DGMDELYKRS-------------------------------------------------
Variant 12  (229) DGMDELYKRS-------------------------------------------------
Variant 13  (229) DGMDELYKRSGTTSLYKKAGSEFALG-------------------------------
Variant 14  (229) DGMDELYKRS-----------------G-----------------------------
Variant 15  (229) DGMDELYKRS-------------------------------------------------
Variant 16  (229) DGMDELYKRS-------------------------------------------------

Section 6
            (286) 286           300       310       320       330       342
Variant 01  (286) LPAERQLAMQLGVSRNSLREALAKLVSEGVLLSRRGGGTFIRWRHDTWSEQNIVQPL
Variant 02  (283) LPSERALSETLGVSRSSLREALRVLEALGTISTATGSGPRSGTIITAAPGQALSLSV
Variant 03  (271) LPAERQLAMQLGVSRNSLREALAKLVSEGVLLSRRGGGTFIRWRHDTWSEQNIVQPL
Variant 04  (268) LPSERALSETLGVSRSSLREALRVLEALGTISTATGSGPRSGTIITAAPGQALSLSV
Variant 05  (286) LPAERQLAMQLGVSRNSLREALAKLVSEGVLLSRRGGGTFIRWRHDTWSEQNIVQPL
Variant 06  (283) LPSERALSETLGVSRSSLREALRVLEALGTISTATGSGPRSGTIITAAPGQALSLSV
Variant 07  (271) LPAERQLAMQLGVSRNSLREALAKLVSEGVLLSRRGGGTFIRWRHDTWSEQNIVQPL
Variant 08  (268) LPSERALSETLGVSRSSLREALRVLEALGTISTATGSGPRSGTIITAAPGQALSLSV
Variant 09  (254) ----------------------------------------------GTEQNIVQPL
Variant 10  (240) --------------------------------TTSLYKKAGSEFALGTGQALSLSV
Variant 11  (239) ------------------------------------------------GTEQNIVQPL
Variant 12  (239) ----------------------------------------------GTGQALSLSV
Variant 13  (255) ------------------------------------------------TEQNIVQPL
Variant 14  (240) --------------------------------TTSLYKKAGSEFALGTGQALSLSV
Variant 15  (239) -----------G----------------------------------TEQNIVQPL
Variant 16  (239) ----------------------------------------------GTGQALSLSV
```

FIGURE 3 (Cont.)

Alignment of Lactate nanosensor variants

Section 7

```
            (343) 343    350        360        370        380               399
Variant 01  (343) KTLMADDPDYSFDILEARYAIEASTAWHAAMRATPGDKEKIQLCFEATLSEDPDIAS
Variant 02  (340) TLQLVTNQVGHHDIYETRQLLEGWAALHSSAERGDWDVAEALLEKMDDPSLPLEDFL
Variant 03  (328) KTLMADDPDYSFDILEARYAIEASTAWHAAMRATPGDKEKIQLCFEATLSEDPDIAS
Variant 04  (325) TLQLVTNQVGHHDIYETRQLLEGWAALHSSAERGDWDVAEALLEKMDDPSLPLEDFL
Variant 05  (343) KTLMADDPDYSFDILEARYAIEASTAWHAAMRATPGDKEKIQLCFEATLSEDPDIAS
Variant 06  (340) TLQLVTNQVGHHDIYETRQLLEGWAALHSSAERGDWDVAEALLEKMDDPSLPLEDFL
Variant 07  (328) KTLMADDPDYSFDILEARYAIEASTAWHAAMRATPGDKEKIQLCFEATLSEDPDIAS
Variant 08  (325) TLQLVTNQVGHHDIYETRQLLEGWAALHSSAERGDWDVAEALLEKMDDPSLPLEDFL
Variant 09  (264) KTLMADDPDYSFDILEARYAIEASTAWHAAMRATPGDKEKIQLCFEATLSEDPDIAS
Variant 10  (264) TLQLVTNQVGHHDIYETRQLLEGWAALHSSAERGDWDVAEALLEKMDDPSLPLEDFL
Variant 11  (249) KTLMADDPDYSFDILEARYAIEASTAWHAAMRATPGDKEKIQLCFEATLSEDPDIAS
Variant 12  (249) TLQLVTNQVGHHDIYETRQLLEGWAALHSSAERGDWDVAEALLEKMDDPSLPLEDFL
Variant 13  (264) KTLMADDPDYSFDILEARYAIEASTAWHAAMRATPGDKEKIQLCFEATLSEDPDIAS
Variant 14  (264) TLQLVTNQVGHHDIYETRQLLEGWAALHSSAERGDWDVAEALLEKMDDPSLPLEDFL
Variant 15  (249) KTLMADDPDYSFDILEARYAIEASTAWHAAMRATPGDKEKIQLCFEATLSEDPDIAS
Variant 16  (249) TLQLVTNQVGHHDIYETRQLLEGWAALHSSAERGDWDVAEALLEKMDDPSLPLEDFL
```

Section 8

```
            (400) 400        410        420        430        440           456
Variant 01  (400) QADVRFHLAIAEASHNIVLLQTMRGFFDVLQSSVKHSRQRMYLVPPVFSQLTEQHQA
Variant 02  (397) RFDAEFHVVISKGAENPLISTLMEALRLSVADHTVARARALPDWRATSARLQKEHRA
Variant 03  (385) QADVRFHLAIAEASHNIVLLQTMRGFFDVLQSSVKHSRQRMYLVPPVFSQLTEQHQA
Variant 04  (382) RFDAEFHVVISKGAENPLISTLMEALRLSVADHTVARARALPDWRATSARLQKEHRA
Variant 05  (400) QADVRFHLAIAEASHNIVLLQTMRGFFDVLQSSVKHSRQRMYLVPPVFSQLTEQHQA
Variant 06  (397) RFDAEFHVVISKGAENPLISTLMEALRLSVADHTVARARALPDWRATSARLQKEHRA
Variant 07  (385) QADVRFHLAIAEASHNIVLLQTMRGFFDVLQSSVKHSRQRMYLVPPVFSQLTEQHQA
Variant 08  (382) RFDAEFHVVISKGAENPLISTLMEALRLSVADHTVARARALPDWRATSARLQKEHRA
Variant 09  (321) QADVRFHLAIAEASHNIVLLQTMRGFFDVLQSSVKHSRQRMYLVPPVFSQLTEQHQA
Variant 10  (321) RFDAEFHVVISKGAENPLISTLMEALRLSVADHTVARARALPDWRATSARLQKEHRA
Variant 11  (306) QADVRFHLAIAEASHNIVLLQTMRGFFDVLQSSVKHSRQRMYLVPPVFSQLTEQHQA
Variant 12  (306) RFDAEFHVVISKGAENPLISTLMEALRLSVADHTVARARALPDWRATSARLQKEHRA
Variant 13  (321) QADVRFHLAIAEASHNIVLLQTMRGFFDVLQSSVKHSRQRMYLVPPVFSQLTEQHQA
Variant 14  (321) RFDAEFHVVISKGAENPLISTLMEALRLSVADHTVARARALPDWRATSARLQKEHRA
Variant 15  (306) QADVRFHLAIAEASHNIVLLQTMRGFFDVLQSSVKHSRQRMYLVPPVFSQLTEQHQA
Variant 16  (306) RFDAEFHVVISKGAENPLISTLMEALRLSVADHTVARARALPDWRATSARLQKEHRA
```

Section 9

```
            (457) 457          470        480        490        500        513
Variant 01  (457) VIDAIFAGDADGARKAMMAHLSFVHTTMKRFDEDQARHARITRLPGEHNEHSREKNA
Variant 02  (454) ILAALRAGESTVAATLIKEHIEGYY--EETAAAEALKKG-------EFDPAFLYKVV
Variant 03  (442) VIDAIFAGDADGARKAMMAHLSFVHTTMKRFDEDQARHARITRLPGEHNEHSREKNA
Variant 04  (439) ILAALRAGESTVAATLIKEHIEGYY--EETAAAEALKKG-------EFDPAFLYKVV
Variant 05  (457) VIDAIFAGDADGARKAMMAHLSFVHTTMKRFDEDQARHARITRLPGEHNEHSREKNA
Variant 06  (454) ILAALRAGESTVAATLIKEHIEGYY--EETAAAEALKR------------------
Variant 07  (442) VIDAIFAGDADGARKAMMAHLSFVHTTMKRFDEDQARHARITRLPGEHNEHSREKNA
Variant 08  (439) ILAALRAGESTVAATLIKEHIEGYY--EETAAAEALKR------------------
Variant 09  (378) VIDAIFAGDADGARKAMMAHLSFVHTTMKRFDEDQARHARITRLPGEHNEHSREKNA
Variant 10  (378) ILAALRAGESTVAATLIKEHIEGYY--EETAAAEALKKG-------EFDPAFLYKVV
Variant 11  (363) VIDAIFAGDADGARKAMMAHLSFVHTTMKRFDEDQARHARITRLPGEHNEHSREKNA
Variant 12  (363) ILAALRAGESTVAATLIKEHIEGYY--EETAAAEALKKG-------EFDPAFLYKVV
Variant 13  (378) VIDAIFAGDADGARKAMMAHLSFVHTTMKRFDEDQARHARITRLPGEHNEHSREKNA
Variant 14  (378) ILAALRAGESTVAATLIKEHIEGYY--EETAAAEALKR------------------
Variant 15  (363) VIDAIFAGDADGARKAMMAHLSFVHTTMKRFDEDQARHARITRLPGEHNEHSREKNA
Variant 16  (363) ILAALRAGESTVAATLIKEHIEGYY--EETAAAEALKR------------------
```

FIGURE 3 (Cont.)

```
Alignment of Lactate nanosensor variants
Section 10
            (514) 514   520        530        540        550        560      570
Variant 01  (514) LKKGEFDPAFLYKVVLKRSTMVSKGEELFTGVVPILVELDGDVNGHKFSVSGEGEGD
Variant 02  (502) LKR---------------STMVSKGEELFTGVVPILVELDGDVNGHKFSVSGEGEGD
Variant 03  (499) LKKGEFDPAFLYKVVLKRSTMVSKGEELFTGVVPILVELDGDVNGHKFSVSGEGEGD
Variant 04  (487) LKR---------------STMVSKGEELFTGVVPILVELDGDVNGHKFSVSGEGEGD
Variant 05  (514) LKR---------------STMVSKGEELFTGVVPILVELDGDVNGHKFSVSGEGEGD
Variant 06  (490) ------------------STMVSKGEELFTGVVPILVELDGDVNGHKFSVSGEGEGD
Variant 07  (499) LKR---------------STMVSKGEELFTGVVPILVELDGDVNGHKFSVSGEGEGD
Variant 08  (475) ------------------STMVSKGEELFTGVVPILVELDGDVNGHKFSVSGEGEGD
Variant 09  (435) LKKGEFDPAFLYKVVLKRSTMVSKGEELFTGVVPILVELDGDVNGHKFSVSGEGEGD
Variant 10  (426) LKR---------------STMVSKGEELFTGVVPILVELDGDVNGHKFSVSGEGEGD
Variant 11  (420) LKKGEFDPAFLYKVVLKRSTMVSKGEELFTGVVPILVELDGDVNGHKFSVSGEGEGD
Variant 12  (411) LKR---------------STMVSKGEELFTGVVPILVELDGDVNGHKFSVSGEGEGD
Variant 13  (435) LKR---------------STMVSKGEELFTGVVPILVELDGDVNGHKFSVSGEGEGD
Variant 14  (414) ------------------STMVSKGEELFTGVVPILVELDGDVNGHKFSVSGEGEGD
Variant 15  (420) LKR---------------STMVSKGEELFTGVVPILVELDGDVNGHKFSVSGEGEGD
Variant 16  (399) ------------------STMVSKGEELFTGVVPILVELDGDVNGHKFSVSGEGEGD

Section 11
            (571) 571      580        590        600        610            627
Variant 01  (571) ATYGKLTLKLICTTGKLPVPWPTLVTTLGYGLQCFARYPDHMKQHDFFKSAMPEGYV
Variant 02  (544) ATYGKLTLKLICTTGKLPVPWPTLVTTLGYGLQCFARYPDHMKQHDFFKSAMPEGYV
Variant 03  (556) ATYGKLTLKLICTTGKLPVPWPTLVTTLGYGLQCFARYPDHMKQHDFFKSAMPEGYV
Variant 04  (529) ATYGKLTLKLICTTGKLPVPWPTLVTTLGYGLQCFARYPDHMKQHDFFKSAMPEGYV
Variant 05  (556) ATYGKLTLKLICTTGKLPVPWPTLVTTLGYGLQCFARYPDHMKQHDFFKSAMPEGYV
Variant 06  (529) ATYGKLTLKLICTTGKLPVPWPTLVTTLGYGLQCFARYPDHMKQHDFFKSAMPEGYV
Variant 07  (541) ATYGKLTLKLICTTGKLPVPWPTLVTTLGYGLQCFARYPDHMKQHDFFKSAMPEGYV
Variant 08  (514) ATYGKLTLKLICTTGKLPVPWPTLVTTLGYGLQCFARYPDHMKQHDFFKSAMPEGYV
Variant 09  (492) ATYGKLTLKLICTTGKLPVPWPTLVTTLGYGLQCFARYPDHMKQHDFFKSAMPEGYV
Variant 10  (468) ATYGKLTLKLICTTGKLPVPWPTLVTTLGYGLQCFARYPDHMKQHDFFKSAMPEGYV
Variant 11  (477) ATYGKLTLKLICTTGKLPVPWPTLVTTLGYGLQCFARYPDHMKQHDFFKSAMPEGYV
Variant 12  (453) ATYGKLTLKLICTTGKLPVPWPTLVTTLGYGLQCFARYPDHMKQHDFFKSAMPEGYV
Variant 13  (477) ATYGKLTLKLICTTGKLPVPWPTLVTTLGYGLQCFARYPDHMKQHDFFKSAMPEGYV
Variant 14  (453) ATYGKLTLKLICTTGKLPVPWPTLVTTLGYGLQCFARYPDHMKQHDFFKSAMPEGYV
Variant 15  (462) ATYGKLTLKLICTTGKLPVPWPTLVTTLGYGLQCFARYPDHMKQHDFFKSAMPEGYV
Variant 16  (438) ATYGKLTLKLICTTGKLPVPWPTLVTTLGYGLQCFARYPDHMKQHDFFKSAMPEGYV

Section 12
            (628) 628          640        650        660        670          684
Variant 01  (628) QERTIFFKDDGNYKTRAEVKFEGDTLVNRIELKGIDFKEDGNILGHKLEYNYNSHNV
Variant 02  (601) QERTIFFKDDGNYKTRAEVKFEGDTLVNRIELKGIDFKEDGNILGHKLEYNYNSHNV
Variant 03  (613) QERTIFFKDDGNYKTRAEVKFEGDTLVNRIELKGIDFKEDGNILGHKLEYNYNSHNV
Variant 04  (586) QERTIFFKDDGNYKTRAEVKFEGDTLVNRIELKGIDFKEDGNILGHKLEYNYNSHNV
Variant 05  (613) QERTIFFKDDGNYKTRAEVKFEGDTLVNRIELKGIDFKEDGNILGHKLEYNYNSHNV
Variant 06  (586) QERTIFFKDDGNYKTRAEVKFEGDTLVNRIELKGIDFKEDGNILGHKLEYNYNSHNV
Variant 07  (598) QERTIFFKDDGNYKTRAEVKFEGDTLVNRIELKGIDFKEDGNILGHKLEYNYNSHNV
Variant 08  (571) QERTIFFKDDGNYKTRAEVKFEGDTLVNRIELKGIDFKEDGNILGHKLEYNYNSHNV
Variant 09  (549) QERTIFFKDDGNYKTRAEVKFEGDTLVNRIELKGIDFKEDGNILGHKLEYNYNSHNV
Variant 10  (525) QERTIFFKDDGNYKTRAEVKFEGDTLVNRIELKGIDFKEDGNILGHKLEYNYNSHNV
Variant 11  (534) QERTIFFKDDGNYKTRAEVKFEGDTLVNRIELKGIDFKEDGNILGHKLEYNYNSHNV
Variant 12  (510) QERTIFFKDDGNYKTRAEVKFEGDTLVNRIELKGIDFKEDGNILGHKLEYNYNSHNV
Variant 13  (534) QERTIFFKDDGNYKTRAEVKFEGDTLVNRIELKGIDFKEDGNILGHKLEYNYNSHNV
Variant 14  (510) QERTIFFKDDGNYKTRAEVKFEGDTLVNRIELKGIDFKEDGNILGHKLEYNYNSHNV
Variant 15  (519) QERTIFFKDDGNYKTRAEVKFEGDTLVNRIELKGIDFKEDGNILGHKLEYNYNSHNV
Variant 16  (495) QERTIFFKDDGNYKTRAEVKFEGDTLVNRIELKGIDFKEDGNILGHKLEYNYNSHNV
```

FIGURE 3 (Cont.)

Alignment of Lactate nanosensor variants

Section 13

	(685)	685 690 700 710 720 730 741
Variant 01	(685)	YITADKQKNGIKANFKIRHNIEDGGVQLADHYQQNTPIGDGPVLLPDNHYLSYQSAL
Variant 02	(658)	YITADKQKNGIKANFKIRHNIEDGGVQLADHYQQNTPIGDGPVLLPDNHYLSYQSAL
Variant 03	(670)	YITADKQKNGIKANFKIRHNIEDGGVQLADHYQQNTPIGDGPVLLPDNHYLSYQSAL
Variant 04	(643)	YITADKQKNGIKANFKIRHNIEDGGVQLADHYQQNTPIGDGPVLLPDNHYLSYQSAL
Variant 05	(670)	YITADKQKNGIKANFKIRHNIEDGGVQLADHYQQNTPIGDGPVLLPDNHYLSYQSAL
Variant 06	(643)	YITADKQKNGIKANFKIRHNIEDGGVQLADHYQQNTPIGDGPVLLPDNHYLSYQSAL
Variant 07	(655)	YITADKQKNGIKANFKIRHNIEDGGVQLADHYQQNTPIGDGPVLLPDNHYLSYQSAL
Variant 08	(628)	YITADKQKNGIKANFKIRHNIEDGGVQLADHYQQNTPIGDGPVLLPDNHYLSYQSAL
Variant 09	(606)	YITADKQKNGIKANFKIRHNIEDGGVQLADHYQQNTPIGDGPVLLPDNHYLSYQSAL
Variant 10	(582)	YITADKQKNGIKANFKIRHNIEDGGVQLADHYQQNTPIGDGPVLLPDNHYLSYQSAL
Variant 11	(591)	YITADKQKNGIKANFKIRHNIEDGGVQLADHYQQNTPIGDGPVLLPDNHYLSYQSAL
Variant 12	(567)	YITADKQKNGIKANFKIRHNIEDGGVQLADHYQQNTPIGDGPVLLPDNHYLSYQSAL
Variant 13	(591)	YITADKQKNGIKANFKIRHNIEDGGVQLADHYQQNTPIGDGPVLLPDNHYLSYQSAL
Variant 14	(567)	YITADKQKNGIKANFKIRHNIEDGGVQLADHYQQNTPIGDGPVLLPDNHYLSYQSAL
Variant 15	(576)	YITADKQKNGIKANFKIRHNIEDGGVQLADHYQQNTPIGDGPVLLPDNHYLSYQSAL
Variant 16	(552)	YITADKQKNGIKANFKIRHNIEDGGVQLADHYQQNTPIGDGPVLLPDNHYLSYQSAL

Section 14

	(742)	742 750 760 772
Variant 01	(742)	SKDPNEKRDHMVLLEFVTAAGITLGMDELYK
Variant 02	(715)	SKDPNEKRDHMVLLEFVTAAGITLGMDELYK
Variant 03	(727)	SKDPNEKRDHMVLLEFVTAAGITLGMDELYK
Variant 04	(700)	SKDPNEKRDHMVLLEFVTAAGITLGMDELYK
Variant 05	(727)	SKDPNEKRDHMVLLEFVTAAGITLGMDELYK
Variant 06	(700)	SKDPNEKRDHMVLLEFVTAAGITLGMDELYK
Variant 07	(712)	SKDPNEKRDHMVLLEFVTAAGITLGMDELYK
Variant 08	(685)	SKDPNEKRDHMVLLEFVTAAGITLGMDELYK
Variant 09	(663)	SKDPNEKRDHMVLLEFVTAAGITLGMDELYK
Variant 10	(639)	SKDPNEKRDHMVLLEFVTAAGITLGMDELYK
Variant 11	(648)	SKDPNEKRDHMVLLEFVTAAGITLGMDELYK
Variant 12	(624)	SKDPNEKRDHMVLLEFVTAAGITLGMDELYK
Variant 13	(648)	SKDPNEKRDHMVLLEFVTAAGITLGMDELYK
Variant 14	(624)	SKDPNEKRDHMVLLEFVTAAGITLGMDELYK
Variant 15	(633)	SKDPNEKRDHMVLLEFVTAAGITLGMDELYK
Variant 16	(609)	SKDPNEKRDHMVLLEFVTAAGITLGMDELYK

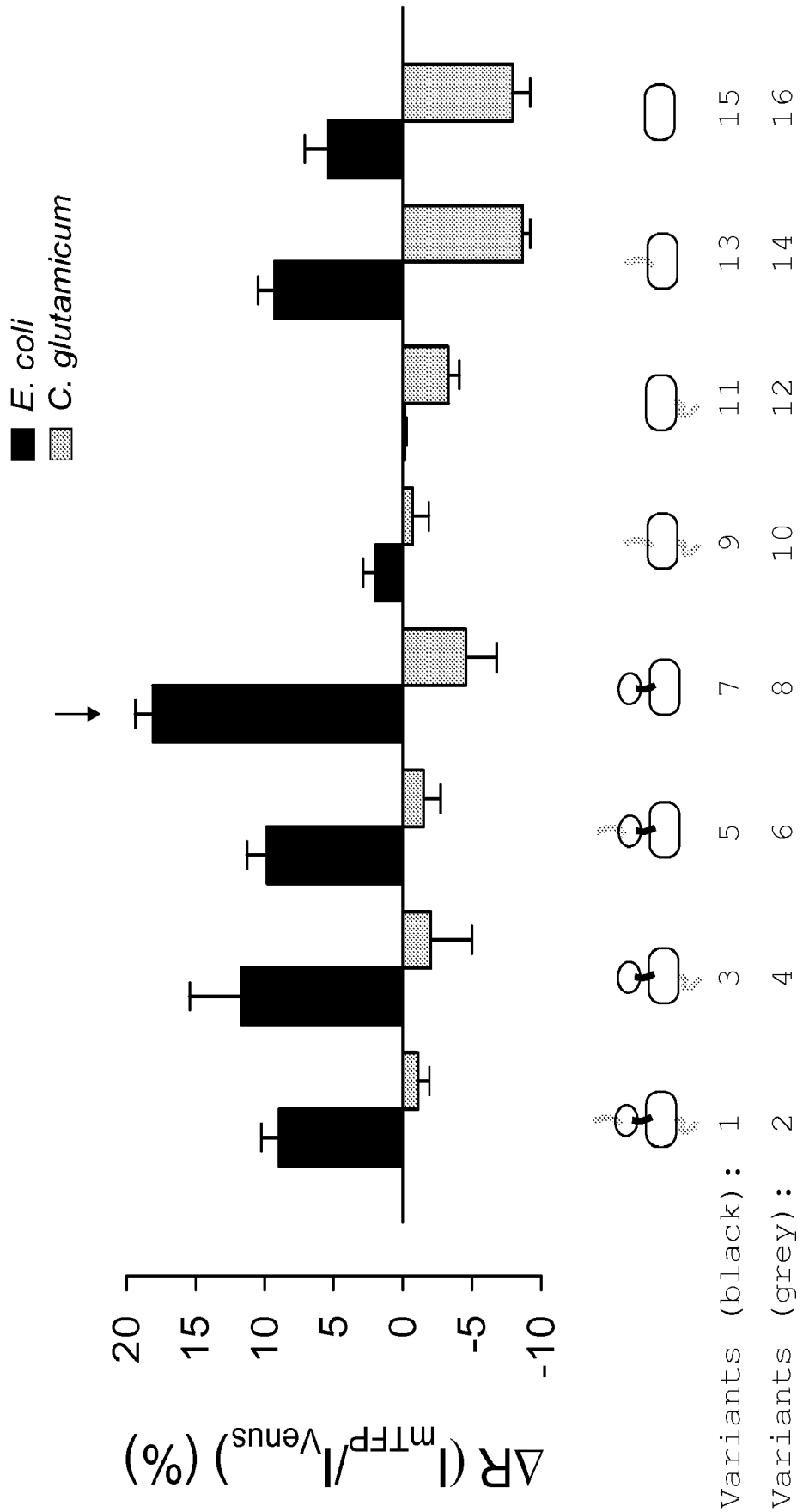
E. coli
C. glutamicum
ΔR (I mTFP/I Venus) (%)
20
15
10
5
0
-5
-10
Variants (black): 1 3 5 7 9 11 13 15
Variants (grey): 2 4 6 8 10 12 14 16

Figure 4

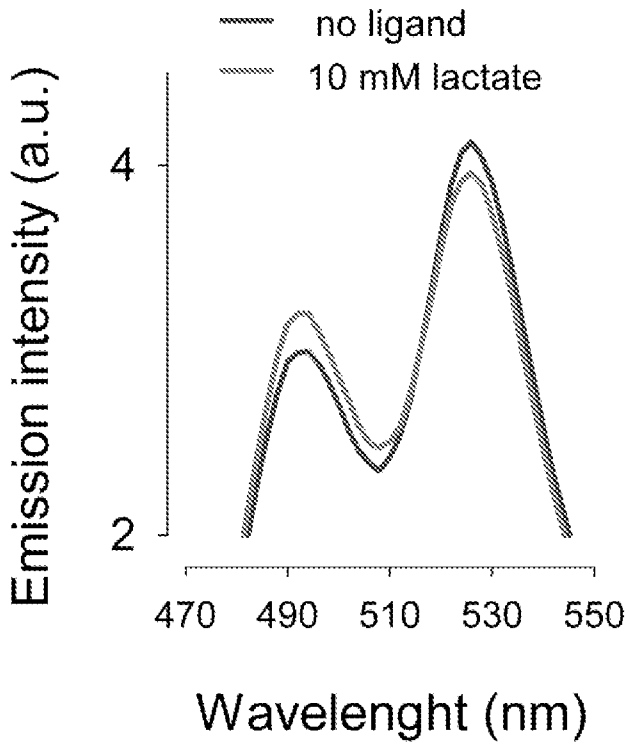
no ligand
10 mM lactate
Emission intensity (a.u.)
4
2
470
490
510
530
550
Wavelenght (nm)

Figure 5

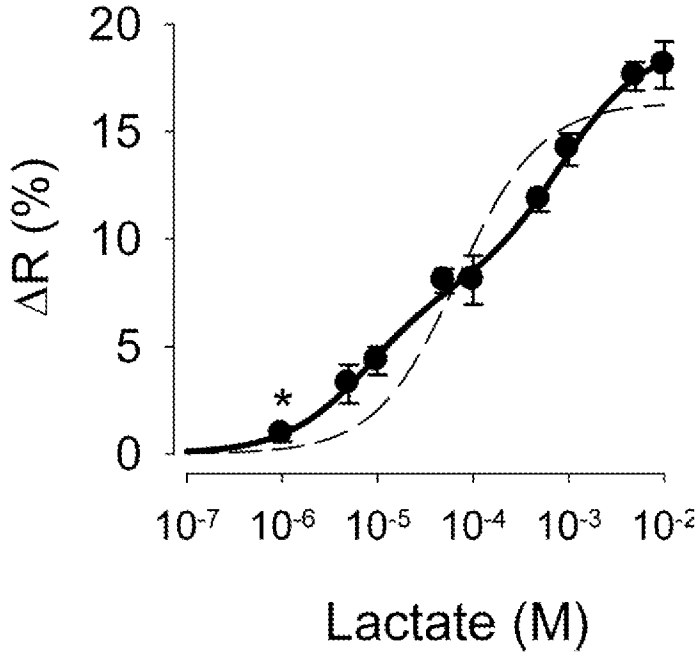

Figure 6

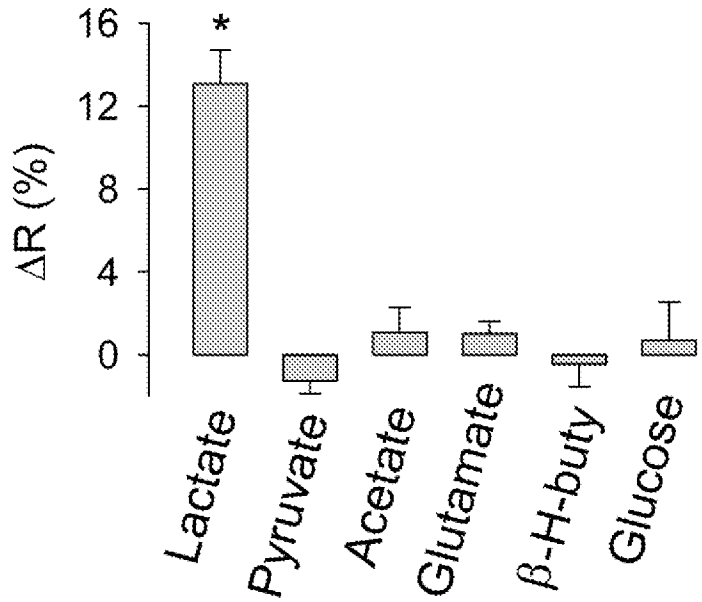

Figure 7

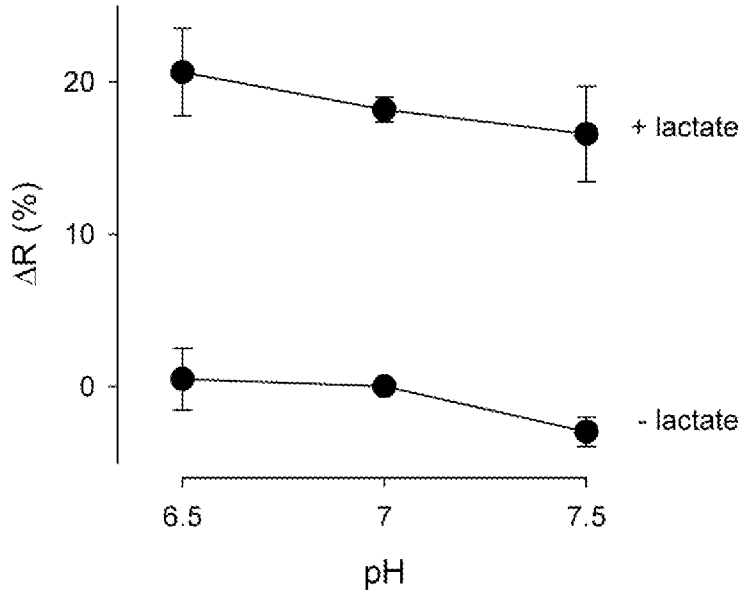

Figure 8

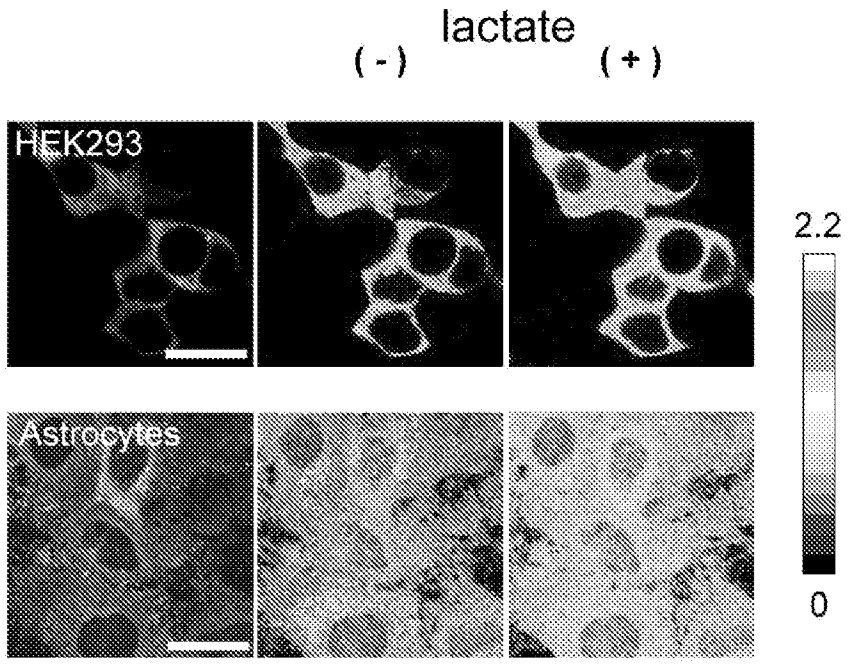

Figure 9

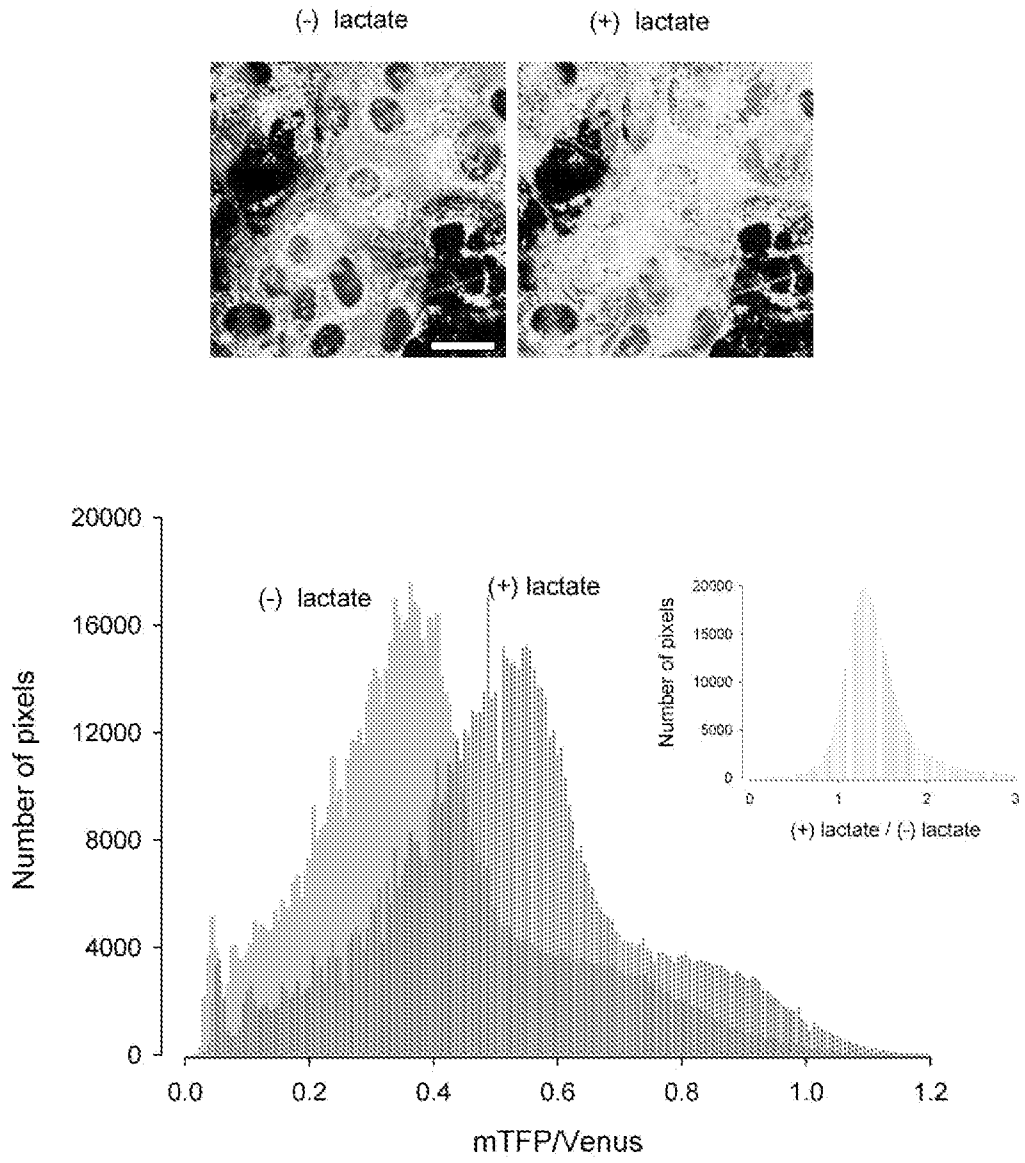
(-) lactate
(+) lactate
20000
16000
12000
8000
4000
0
Number of pixels
(-) lactate
(+) lactate
0.0
0.2
0.4
0.6
0.8
1.0
1.2
mTFP/Venus
20000
15000
10000
5000
0
Number of pixels
0
1
2
3
(+) lactate / (-) lactate

Figure 10

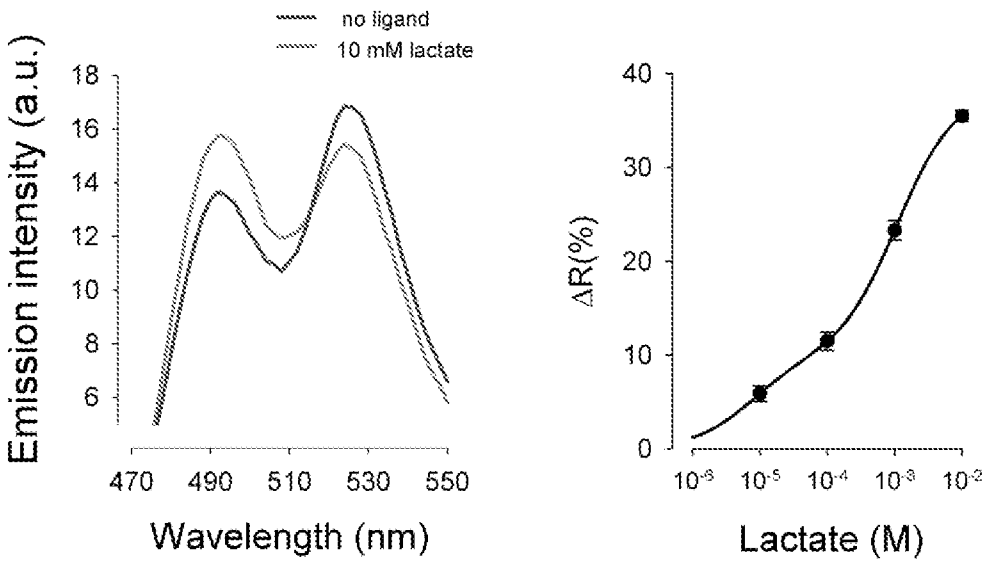
no ligand
10 mM lactate
Emission intensity (a.u.)
18
16
14
12
10
8
6
470
490
510
530
550
Wavelength (nm)
ΔR(%)
40
30
20
10
0
10-6
10-5
10-4
10-3
10-2
Lactate (M)

Figure 11

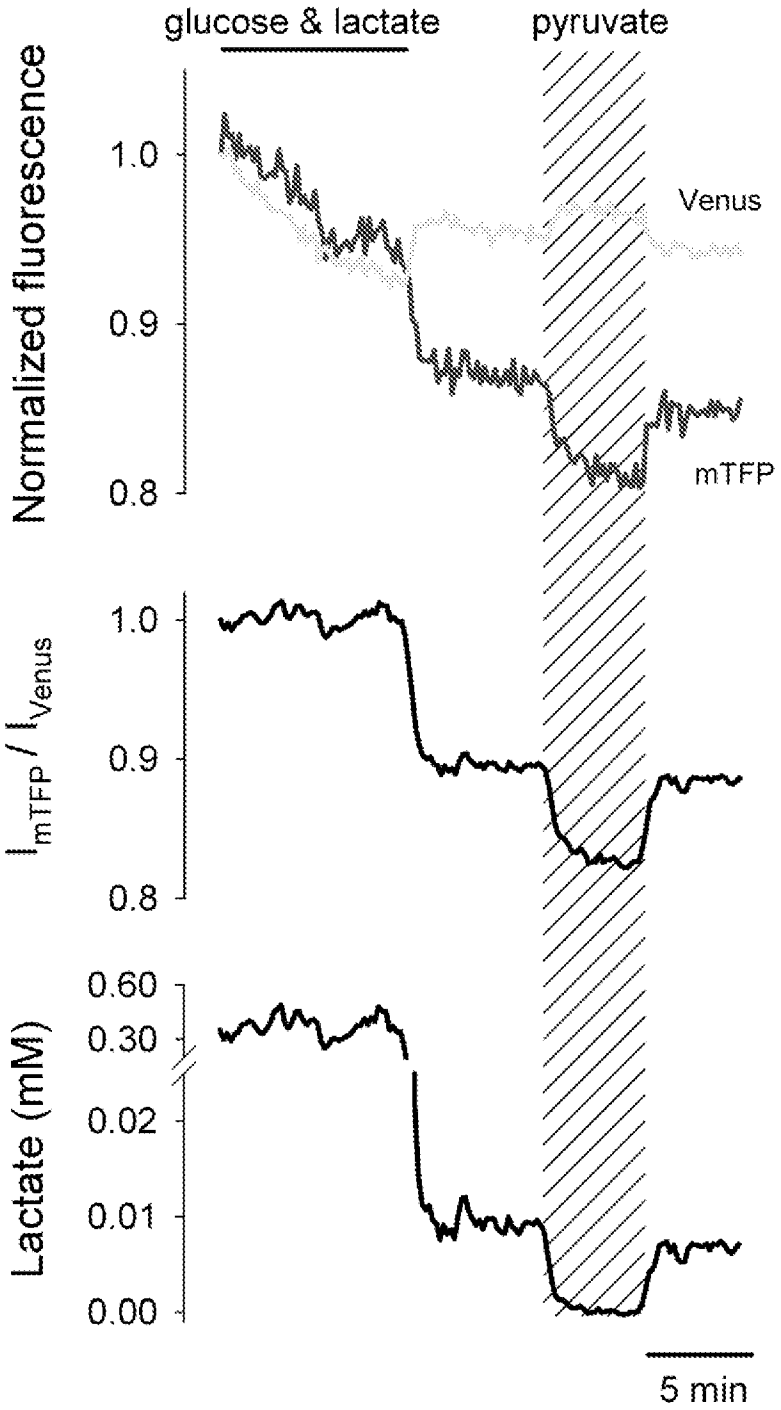
glucose & lactate
pyruvate
Normalized fluorescence
1.0
0.9
0.8
Venus
mTFP
I_{mTFP} / I_{Venus}
1.0
0.9
0.8
Lactate (mM)
0.60
0.30
0.02
0.01
0.00
5 min

Figure 12

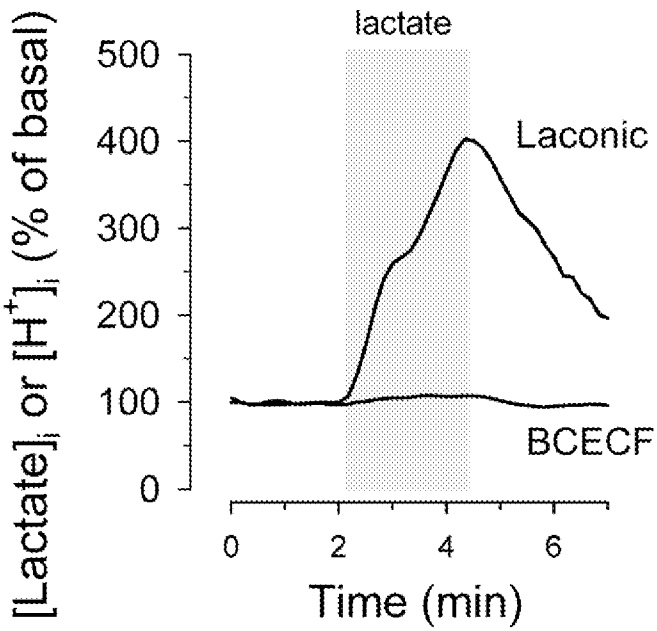
lactate
Laconic
BCECF
[Lactate]$_i$ or [H^+]$_i$ (% of basal)
500
400
300
200
100
0
0
2
4
6
Time (min)

Figure 13

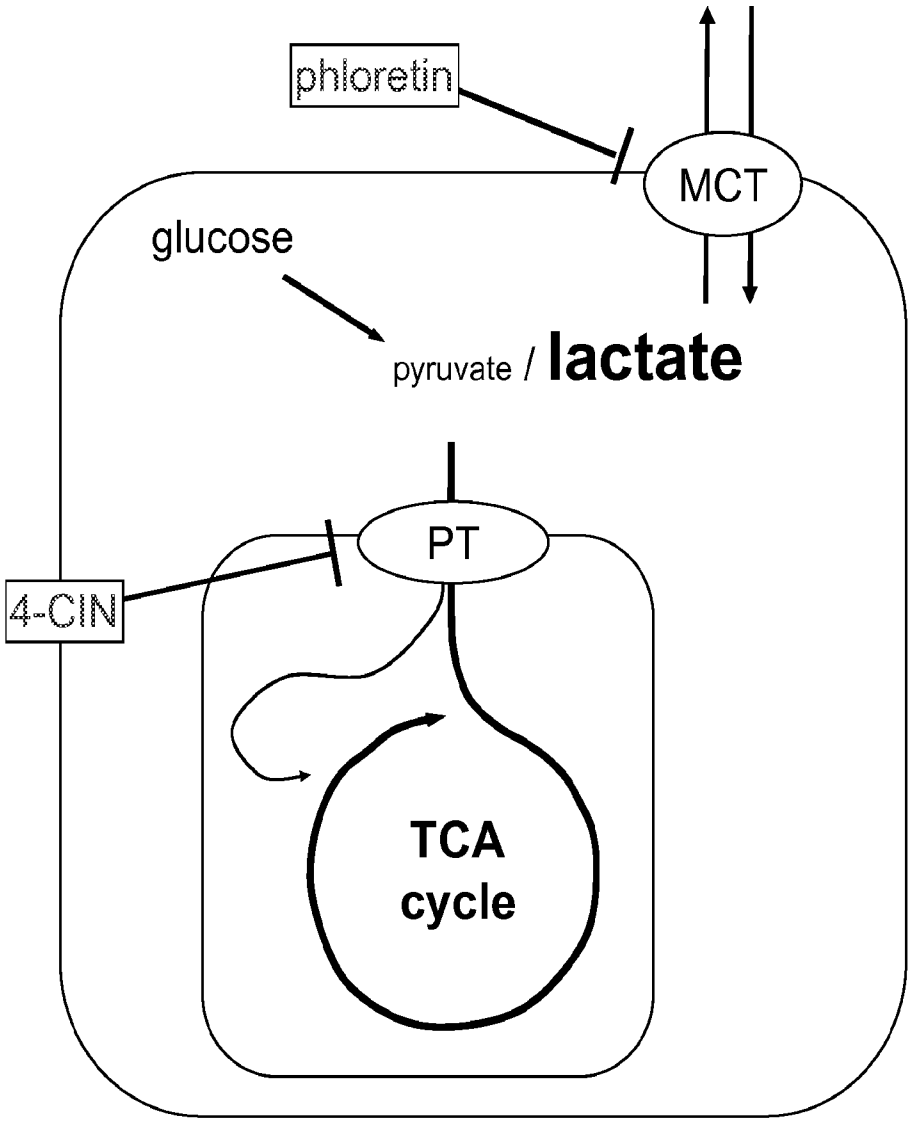

Figure 14

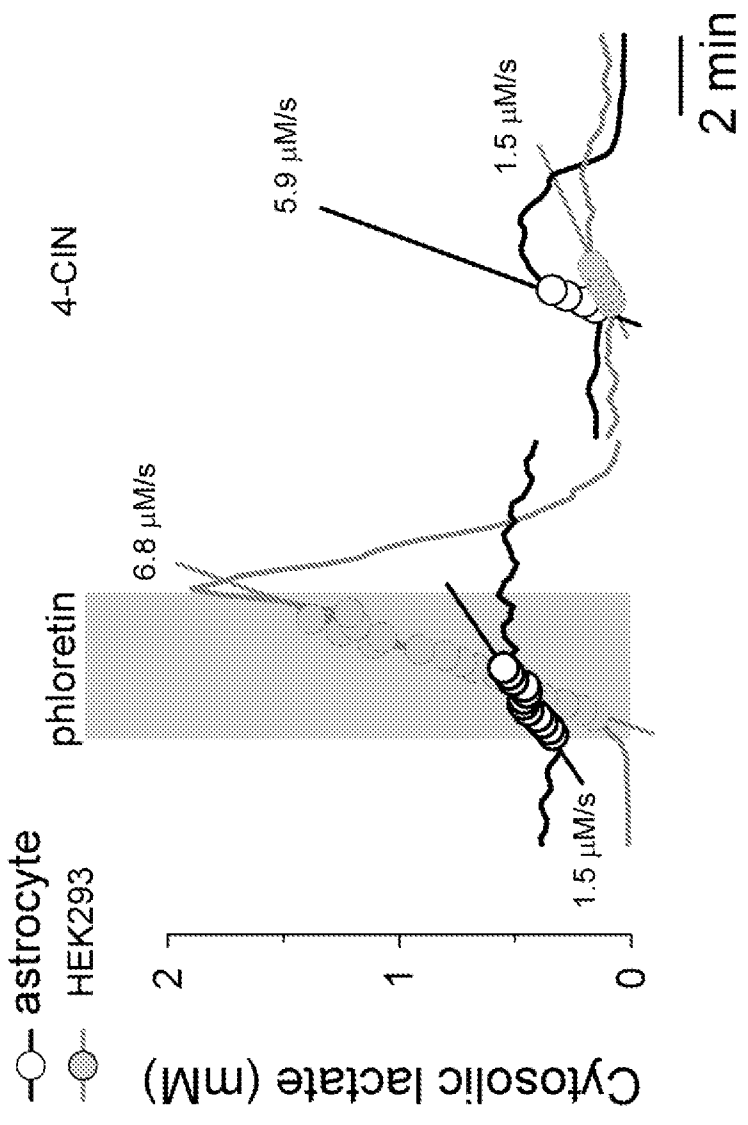
astrocyte
HEK293
Cytosolic lactate (mM)
2
1
0
phloretin
4-CIN
6.8 μM/s
5.9 μM/s
1.5 μM/s
1.5 μM/s
2 min

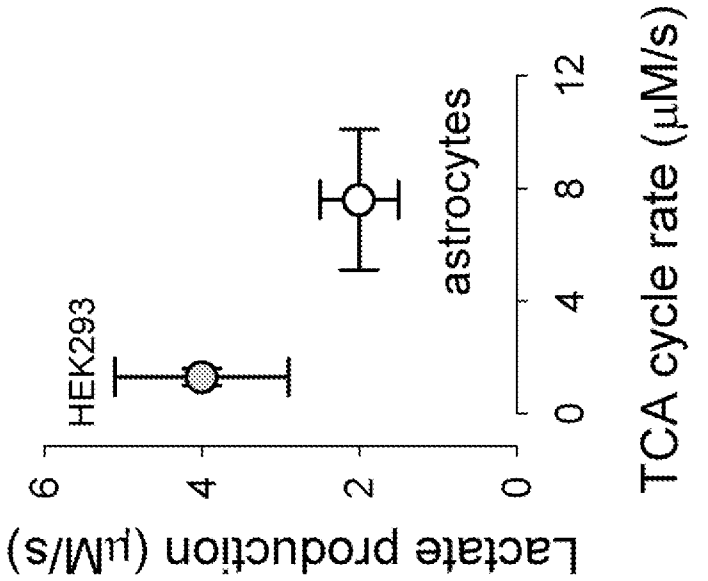
Lactate production (μM/s)
6
4
2
0
HEK293
astrocytes
0
4
8
12
TCA cycle rate (μM/s)

Figure 15

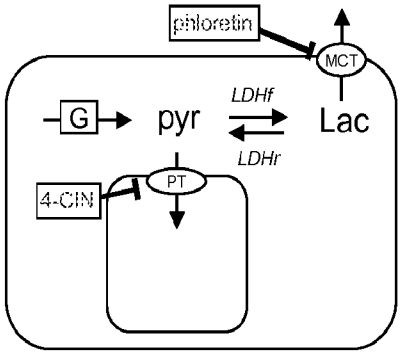

Pyruvate concentration, [Pyr] (μM)
Lactate, [Lac] (μM)
Glycolytic pyruvate production, G (μM/s)
Lactate dexydrogenase forward reaction, *LDHf* (s^{-1})
Lactate dehydrogenase reverse reaction, *LDHr* (s^{-1})
Cellular lactate release, MCT (μM/s)
Mitochondrial pyruvate uptake, PT (μM/s)

Equations

$d[Pyr]/dt = (G + [Lac]*LDHr - [Pyr]*LDHf - PT)/vol$

$d[Lac]/dt = ([Pyr]*LDHf - [Lac]*LDHr - MCT)/vol$

$MCT=V_{MCT}*[Lac]/(K_{MCT} + [Lac])$

$K_{MCT} = 5000$; Vol=1liter

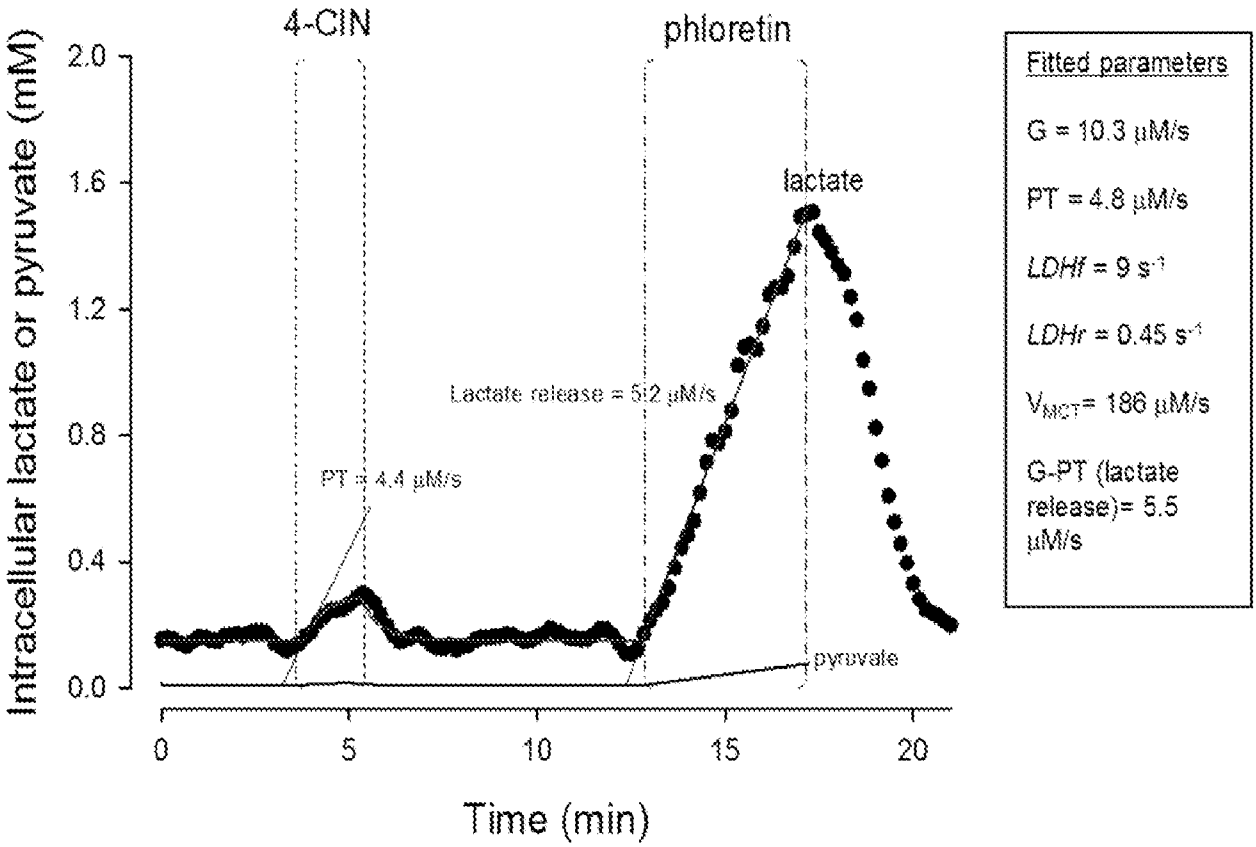

Fitted parameters

G = 10.3 μM/s

PT = 4.8 μM/s

LDHf = 9 s^{-1}

LDHr = 0.45 s^{-1}

V_{MCT} = 186 μM/s

G-PT (lactate release)= 5.5 μM/s

Figure 16

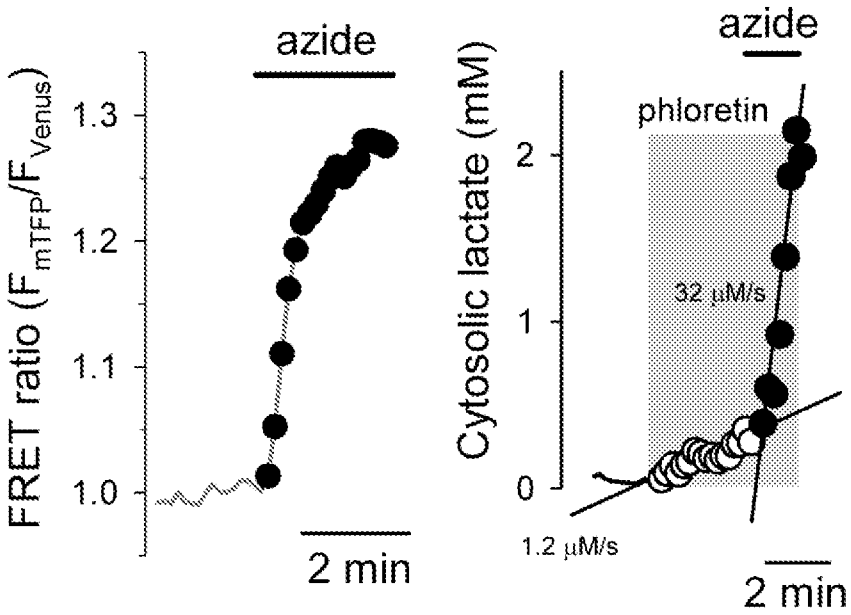
azide
FRET ratio (F_{mTFP}/F_{Venus})
1.3
1.2
1.1
1.0
2 min
azide
phloretin
Cytosolic lactate (mM)
2
1
0
32 μM/s
1.2 μM/s
2 min

Figure 17

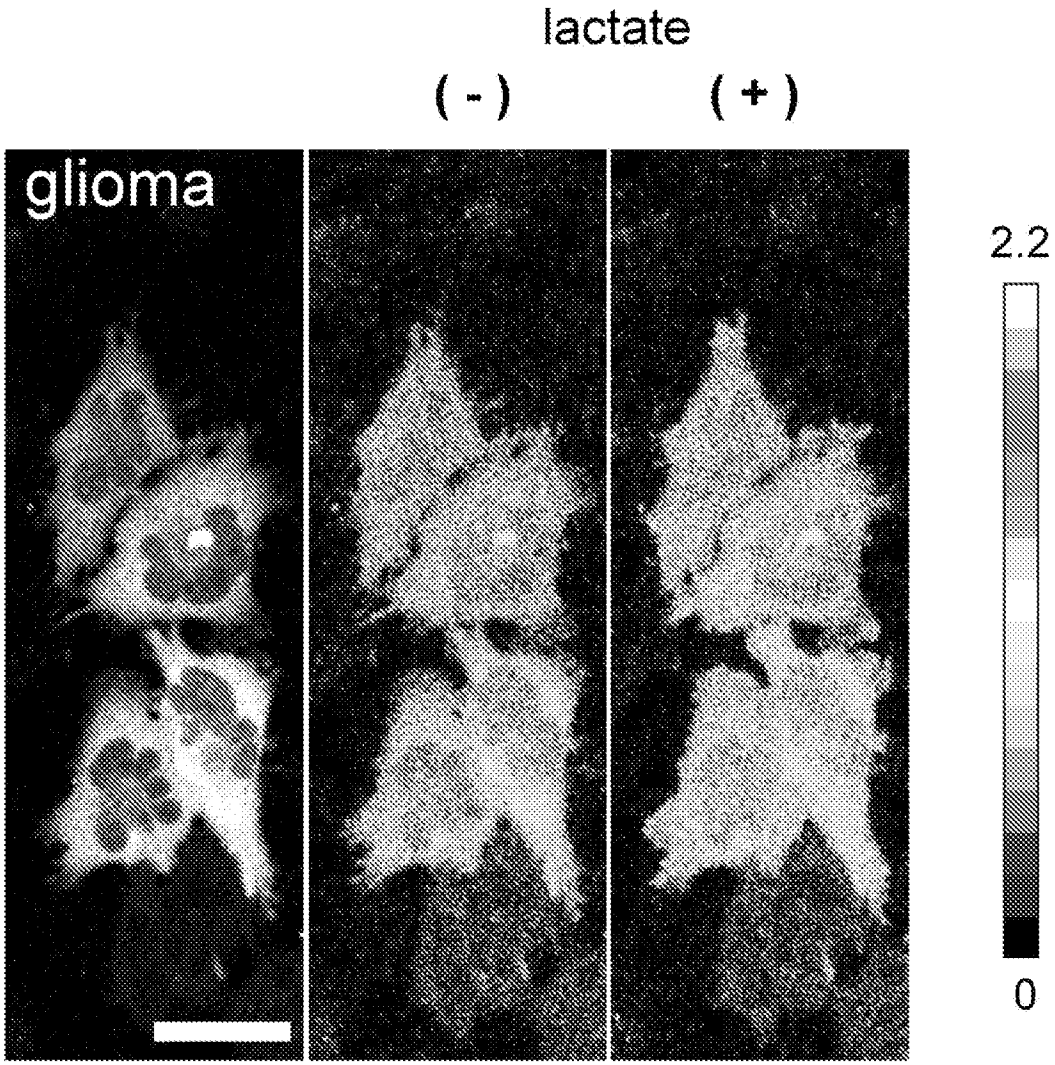

Figure 18

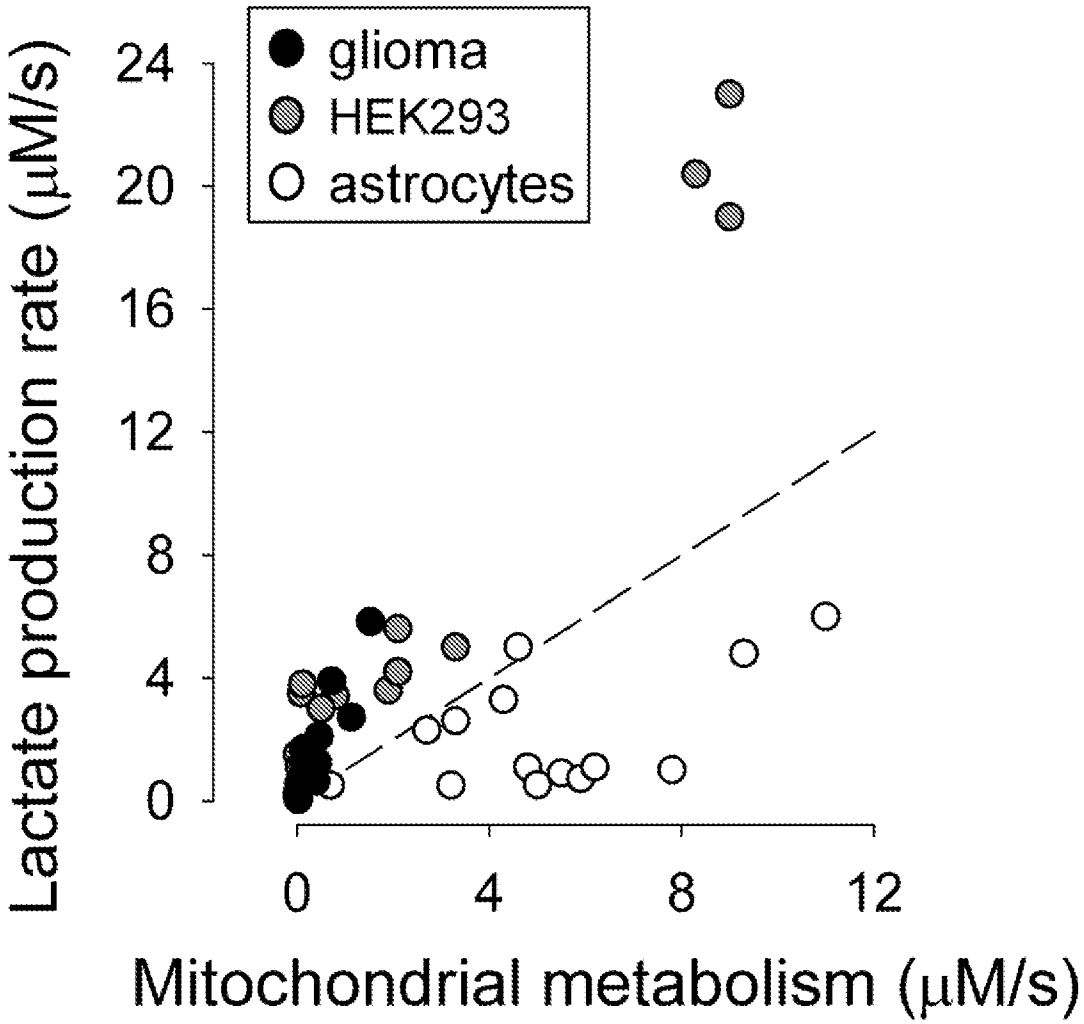
glioma
HEK293
astrocytes
Lactate production rate (μM/s)
24
20
16
12
8
4
0
0
4
8
12
Mitochondrial metabolism (μM/s)

Figure 19

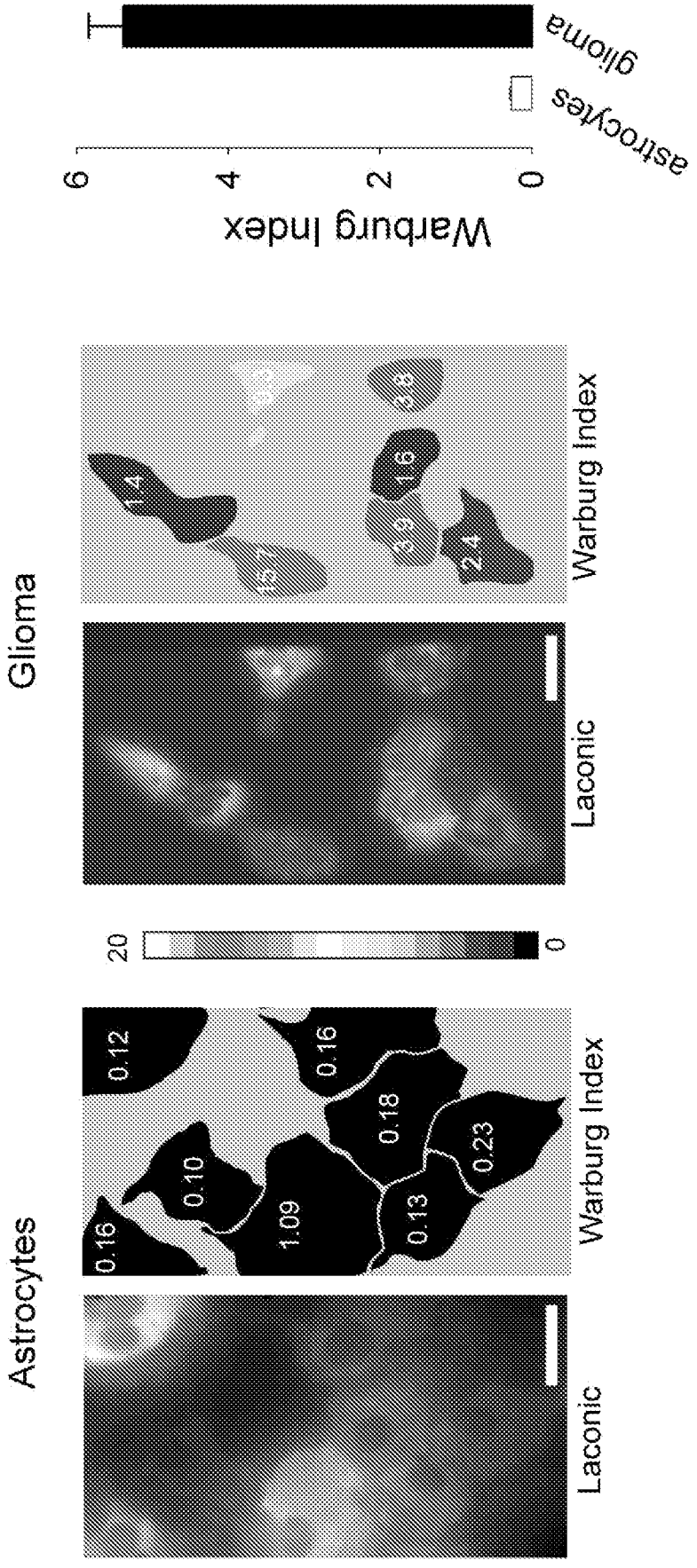
Warburg Index
0
2
4
6
astrocytes
glioma
Glioma
Warburg Index
Laconic
20
0
Astrocytes
Warburg Index
Laconic
0.12
0.16
0.10
0.16
0.18
0.23
0.13
1.09
1.4
15.1
3.9
1.6
2.4

Figure 20

INTERNATIONAL SEARCH REPORT

International application No.
PCT/US 12/33639

A. CLASSIFICATION OF SUBJECT MATTER
IPC(8) - C07K 1/00; C07H 21/04; C12N 5/00 (2013.01)
USPC - 530/350; 536/23.4; 435/325
According to International Patent Classification (IPC) or to both national classification and IPC

B. FIELDS SEARCHED

Minimum documentation searched (classification system followed by classification symbols)
IPC(8) - C07K 1/00; C07H 21/04; C12N 5/00; C12N 15/00 (2013.01) - see keyword below
USPC - 530/350; 536/23.4; 435/325; 435/320.1 - see keyword below

Documentation searched other than minimum documentation to the extent that such documents are included in the fields searched
IPC(8) - C07K 1/00; C07H 21/04; C12N 5/00; C12N 15/00 (2013.01) - see keyword below
USPC - 530/350; 536/23.4; 435/325; 435/320.1 - see keyword below

Electronic data base consulted during the international search (name of data base and, where practicable, search terms used)
PubWEST(USPT,PGPB,EPAB,JPAB); PatBase; Medline, Google: Forster resonance energy transfer, FRET, lactate, nanosensor, monocarboxylate, LIDR, donor, acceptor, mTFP, monomeric teal fluorescent protein, CFP, cyan fluorescent protein, BFP, blue fluorescent protein, GFP, green fluorescent protein, YFP, yellow fluorescent protein, enhanced YFP, EYFP, Y

C. DOCUMENTS CONSIDERED TO BE RELEVANT

Category*	Citation of document, with indication, where appropriate, of the relevant passages	Relevant to claim No.
Y --- A	US 2009/0188001 A1 (FROMMER et al.) 23 July 2009 (23.07.2009), Abstract, para [0003], [0008], [0016], [0017], [0030], [0033], [0035], [0038], [0041], [0043], and [0053]	1-3 ----- 4-17
Y --- A	AGUILERA et al. Dual Role of LldR in Regulation of the lldPRD Operon, Involved in L-Lactate Metabolism in Escherichia coli. J Bacteriol. 2008, Vol. 190(8), p. 2997-3005. Abstract; pg 3000, Fig 2; pg 3003, col 2, para 1; and pg 3004, col 1, last para	1-3 ----- 4-17
Y --- A	US 2006/0275827 A1 (CAMPBELL et al.) 07 December 2006 (07.12.2006), Abstract, para [0002], [0030], [0115], [0118], and SEQ ID NO: 7	1-3 ----- 4-17
Y --- A	UniProt_P0ACL7, Putative L-lactate dehydrogenase operon regulatory protein, Last modified: 22 November 2005 [online]. [Retrieved on 2012.07.13]. Retrieved from the Internet: <URL: http://www.uniprot.org/uniprot/P0ACL7> Gene Name; and Sequence	1-3 ----- 4-17
Y --- A	US 2003/0017538 A1 (MIYAWAKI et al.) 23 January 2003 (23.01.2003), para [0010], [0013], [0014], [0102], and SEQ ID NO: 1	1-3 ----- 4-17
Y --- A	US 2003/0100707 A1 (HWANG et al.) 29 May 2003 (29.05.2003), para [0224], and SEQ ID NO: 76	1-3 ----- 4-17
Y --- A	GenBank_HQ456316, Retroviral Tet-shRNA expression vector TRMPV-ns, complete sequence, 11 December 2010 [online]. [Retrieved on 2013.01.27]. Retrieved from the Internet: <URL: http://www.ncbi.nlm.nih.gov/nuccore/HQ456316> Definition; and Origin	1-3 ----- 4-17

☒ Further documents are listed in the continuation of Box C. ☐

* Special categories of cited documents:
"A" document defining the general state of the art which is not considered to be of particular relevance
"E" earlier application or patent but published on or after the international filing date
"L" document which may throw doubts on priority claim(s) or which is cited to establish the publication date of another citation or other special reason (as specified)
"O" document referring to an oral disclosure, use, exhibition or other means
"P" document published prior to the international filing date but later than the priority date claimed
"T" later document published after the international filing date or priority date and not in conflict with the application but cited to understand the principle or theory underlying the invention
"X" document of particular relevance; the claimed invention cannot be considered novel or cannot be considered to involve an inventive step when the document is taken alone
"Y" document of particular relevance; the claimed invention cannot be considered to involve an inventive step when the document is combined with one or more other such documents, such combination being obvious to a person skilled in the art
"&" document member of the same patent family

Date of the actual completion of the international search	Date of mailing of the international search report
26 January 2013 (26.01.2013)	26 FEB 2013
Name and mailing address of the ISA/US Mail Stop PCT, Attn: ISA/US, Commissioner for Patents P.O. Box 1450, Alexandria, Virginia 22313-1450 Facsimile No. 571-273-3201	Authorized officer: Lee W. Young PCT Helpdesk: 571-272-4300 PCT OSP: 571-272-7774

Form PCT/ISA/210 (second sheet) (July 2009)

INTERNATIONAL SEARCH REPORT

International application No.
PCT/US 12/33639

C (Continuation). DOCUMENTS CONSIDERED TO BE RELEVANT

Category*	Citation of document, with indication, where appropriate, of the relevant passages	Relevant to claim No.
A	US 2009/0126034 A1 (FROMMER et al.) 14 May 2009 (14.05.2009), para [0017], [0047], [0049], [0059], and [0062]	1-17
A	LOOGER et al. Computational design of receptor and sensor proteins with novel functions. Nature. 2003, Vol. 423(6936), p.185-90. Abstract; pg 186, Fig 1; and pg 189, col 1, up para, col 2, and Fig 3	1-17
A	OKUMOTO et al. Quantitative Imaging with Fluorescent Biosensors. Annu Rev Plant Biol. 2012 June, Vol. 63, p. 663-706. Epub 2012 Feb 13. pg 862, col 2, last para; and pg 863, col 1, top para	1-17
A	EKBERG et al. Analyte Flux at a Biomaterial-Tissue Interface over Time: Implications for Sensors for Type 1 and 2 Diabetes Mellitus. J Diabetes Sci Technol. 2010, Vol. 4(5), p. 1063-72. Abstract; pg 1064, col 2, and Fig 1	1-17
A	SCOTT et al. Comparative Metabolic Flux Profiling of Melanoma Cell Lines BEYOND THE WARBURG EFFECT. J Biol Chem. 2011, Vol. 286(49), p. 42626-34. Epub 2011 Oct 13. Abstract	1-17
A	PHILP et al. Lactate - a signal coordinating cell and systemic function. J Exp Biol. 2005, Vol. 208(Pt 24), p. 4561-75. Abstract	1-17
A	KOMATSU et al. Development of an optimized backbone of FRET biosensors for kinases and GTPases. Mol Biol Cell. 2011 Dec, Vol. 22(23), p. 4647-56. Epub 2011 Oct 5. Entire documentation, especailly Abstract; pg 4648, Fig 1; and pg 4649, Fig 2	1-17
A	LOOGER et al. Genetically Encoded FRET Sensors for Visualizing Metabolites with Subcellular Resolution in Living Cells. Plant Physiol. 2005, Vol. 138(2), p. 555-557. Entire documentation	1-17

INTERNATIONAL SEARCH REPORT

International application No.
PCT/US 12/33639

Box No. II Observations where certain claims were found unsearchable (Continuation of item 2 of first sheet)

This international search report has not been established in respect of certain claims under Article 17(2)(a) for the following reasons:

1. ☐ Claims Nos.:
because they relate to subject matter not required to be searched by this Authority, namely:

2. ☐ Claims Nos.:
because they relate to parts of the international application that do not comply with the prescribed requirements to such an extent that no meaningful international search can be carried out, specifically:

3. ☐ Claims Nos.:
because they are dependent claims and are not drafted in accordance with the second and third sentences of Rule 6.4(a).

Box No. III Observations where unity of invention is lacking (Continuation of item 3 of first sheet)

This International Searching Authority found multiple inventions in this international application, as follows:
This application contains the following inventions or groups of inventions which are not so linked as to form a single general inventive concept under PCT Rule 13.1. In order for all inventions to be examined, the appropriate additional examination fees must be paid.

Group I, claims 1-5, drawn to a Forster Resonance Energy Transfer (FRET)-based lactate nanosensor comprising a bacterial LldR transcription factor between any suitable donor and acceptor fluorescent proteins moieties that are capable in combination of serving as donor and acceptor moieties in FRET, which can be expressed in single cells or cell populations, adherent cells or in suspension, in a cell culture, a tissue culture, a mixed cell culture, a tissue explant, or in animal tissues in vivo.

**********Continued in the supplemental box**********

1. ☒ As all required additional search fees were timely paid by the applicant, this international search report covers all searchable claims.

2. ☐ As all searchable claims could be searched without effort justifying additional fees, this Authority did not invite payment of additional fees.

3. ☐ As only some of the required additional search fees were timely paid by the applicant, this international search report covers only those claims for which fees were paid, specifically claims Nos.:

4. ☐ No required additional search fees were timely paid by the applicant. Consequently, this international search report is restricted to the invention first mentioned in the claims; it is covered by claims Nos.:

Remark on Protest

☐ The additional search fees were accompanied by the applicant's protest and, where applicable, the payment of a protest fee.

☐ The additional search fees were accompanied by the applicant's protest but the applicable protest fee was not paid within the time limit specified in the invitation.

☒ No protest accompanied the payment of additional search fees.

Continuation of:
Box No III (unity of invention is lacking)

Group II, claims 6-17, drawn to a method for the measurement of lactate, a method for the measurement of the rate of lactate production or consumption, a method for the measurement of the rate of mitochondrial pyruvate
consumption, or a method for the quantification of the Warburg phenomenon wherein the method comprises the steps of: a. Expressing a FRET-based, lactate nanosensor in a desired host, recording the output from the nanosens or calculating the lactate concentration at different time points and determining the rates of transport, as indicated in claims 6, 9, 12, or 15.

The inventions listed as Groups I-II do not relate to a single general inventive concept under PCT Rule 13.1 because, under PCT Rule 13.2, they lack the same or corresponding special technical features for the following reasons:

Group I does not include the inventive concept of recording the output from the nanosensor calculating the lactate concentration at different time points and determining the rates of transport, as required by Group II.

The inventions of Groups I and II share the technical feature of a FRET-based lactate nanosensor which can be expressed in single cells or cell populations, adherent cells or in suspension, in a cell culture, a tissue culture, a mixed cell culture, a tissue explant, or in animal tissues in vivo. However, this shared technical feature does not represent a contribution over prior art as being obvious over US 2009/0188001 A1 to Frommer et al. (hereinafter 'Frommer'), in view of an article entitled 'Dual Role of LldR in Regulation of the lldPRD Operon, Involved in L-Lactate Metabolism in Escherichia coli' by AGUILERA et al. (hereinafter 'Aguilera'; J Bacteriol. 2008 April; 190(8): 2997-3005), and further in view of US 2006/0275827 A1 to CAMPBELL et al. (hereinafter 'Campbell'), UniProtKB accession number P0ACL7 (hereinafter 'UniProt_P0ACL7'), and US 2003/0017538 A1 to MIYAWAKI et al. (hereinafter 'Miyawaki') as follows:

Frommer discloses a Forster Resonance Energy Transfer (FRET)-based metabolite nanosensor (para [0003] - 'sucrose biosensors and methods for measuring and detecting changes in sucrose levels using fluorescence resonance energy transfer (FRET)', wherein 'sucrose' is 'a metabolite, and 'sucrose biosensors...detecting changes in sucrose levels using fluorescence resonance energy transfer (FRET)' is 'Forster Resonance Energy Transfer (FRET)-based metabolite nanosensor'; para [0017] - 'the sucrose sensor including substrate-induced FRET changes of nanosensors ...fluorescent sucrose nanosensor')
---comprising a metabolite binding protein between any suitable donor and acceptor fluorescent proteins moieties that are capable in combination of serving as donor and acceptor moieties in FRET (para [0053] - 'sucrose binding protein (SmThuE) To generate a sucrose sensor, SmThuE was fused with two GFP variants by attaching a cyan (CFP) and a yellow fluorescent protein (YFP) to the N- and C-termini of the binding protein', wherein 'sucrose binding protein (SmThuE)' is ' a metabolite binding protein' that binds to the metabolite - sucrose, and wherein 'CFP' is 'a FRET donor' and 'YFP' is 'an acceptor fluorescent protein'; para [0030] - 'the donor/acceptor pair CFP/YFP Venus'),
--- which can be expressed in single cells or cell populations, adherent cells or in suspension, in a cell culture, a tissue culture, a mixed cell culture, a tissue explant, or in animal tissues in vivo (para [0035] - 'The sucrose biosensors ... may be expressed in any location in the cell'; para [0016] - 'provides sucrose biosensors ... detecting and measuring changes in sucrose concentrations in living cells'; para [0038] - 'host cells transfected with a vector... animal cells or plant cells. ...plant cell tissue cultures ...a transgenic non-human animal having a phenotype characterized by expression of the nucleic acid sequence coding for the expression of the environmentally stable biosensor'; para [0041] - 'for detecting sucrose binding and measuring changes in the levels of sucrose both in vitro and in a plant or an animal. ...(a) providing a cell expressing a nucleic acid encoding a sucrose biosensor ...wherein a change in FRET between said donor moiety and said acceptor moiety indicates a change in the level of sucrose in the sample of cells'). Frommer further discloses the key for the metabolite sensor is it comprises a metabolite binding domain (Abstract - 'a sucrose binding domain conjugated to donor and fluorescent moieties that permit detection and measurement of Fluorescence Resonance Energy Transfer upon sucrose binding'; para [0008] - 'The development of genetically encoded molecular sensors, ... The recognition element may simply bind the target').
Frommer dose not specifically teach wherein the FRET-based metabolite nanosensor is a FRET-based lactate nanosensor comprising a bacterial LldR transcription factor for binding lactate. Aguilera discloses a bacterial LldR transcription factor comprising a lactate binding domain (Abstract - 'The lldPRD operon of Escherichia coli, involved in L-lactate metabolism ... induction of an lldP-lacZ fusion by L-lactate is lost in an del.lldR mutant, indicating the role of LldR in this induction ...transcriptional level. ... LldR has a dual role, acting as a repressor or an activator of lldPRD...Binding of L-lactate to LldR promotes a conformational change', wherein 'LldR' from 'lldPRD operon of Escherichia coli...LldR has a dual role, acting as a repressor or an activator of lldPRD ' indicating 'LldR' is 'a bacterial LldR transcription factor' and further wherein 'Binding of L-lactate to LldR promotes a conformational change' indicating LldR comprising a lactate binding domain; pg 3000, Fig 2; pg 3003, col 2, para 1 - the activation mediated by LldR in the presence of L-lactate'; pg 3004, col 1, last para - 'When L-lactate is present, binding of this effector molecule to the C-terminal domain of LldR promotes a conformational change'). One of ordinary skill in the art at the time the invention was made would have been motivated to combine the teachings of Aguilera and Frommer to produce a Forster Resonance Energy Transfer (FRET)-based lactate nanosensor comprising a bacterial LldR transcription factor, by replacing the metabolite binding protein in the FRET-based metabolite nanosensor taught by Frommer with the bacterial LldR transcription factor taught by Aguilera for detecting lactate level with expected success, because lactate is an important biological metabolite (Please see: an article entitled by 'Lactate - a signal coordinating cell and systemic function' by Philp et al.: Abstract), and an effort for generating a biosensor for detecting the level of lactate with a different approach has been reported (please see: Looger et al. Abstract - 'to construct soluble receptors that bind... L-lactate ... with high selectivity and affinity. These engineered receptors can function as biosensors for their new ligands'; pg pg 189, col 2 - 'Elevated concentrations of L-lactate are indicative of several medical conditions'; and Fig 3).
Furthermore, Campbell discloses a fluorescent protein mTFP1 sequence ([0030] - 'the complete protein sequence of mTFP1 (SEQ ID NO: 7)'), which is 100% identical to amino acid residues 1-236 of the claimed SEQ ID NO: 1.
UniProt_P0ACL7 discloses discloses a LldR protein sequence (Gene names - 'Name: lldR'; sequence ? 258 a.a), which is 100% identical to the amino acid residues 256-513 of the claimed SEQ ID NO: 1.
**********Continued in the next extra sheet**********

Continuation of:
The previous extra sheet - Box No III (unity of invention is lacking)

(Continuaiton of the discussion for Group I and II)

Miyawaki discloses various of fluorescent proteins used as an acceptor for FRET including a YFP protein sequence (para [0010] - 'the present inventors have carried out concentrated research and have constructed a novel mutant of YFP. .... by using it as an acceptor for immediate detection of reliable FRET (fluorescence resonance energy transfer) signals'; para [0102] - 'the fluorescent protein of the present invention is a mutant of the yellow fluorescent protein (YFP), the fluorescent protein of the present invention is used as an acceptor molecule (para [0013] -[0014] - 'the fluorescent protein having any of the following sequences; ...(a) an amino acids sequence shown in SEQ ID NO: 1'), which is 100% identical to the amino acid residues of 534-772 of the claimed SEQ ID NO:1.

It would have been obvious to one of ordinary skill in the art at the time the invention was made to combine the teachings of Frommer, Aguilera, Campbell, UniProt_P0ACL7, and Miyawaki, to obtain a Forster Resonance Energy Transfer (FRET)-based metabolite nanosensor comprising a metabolite binding protein between any suitable donor and acceptor fluorescent proteins moieties that are capable in combination of serving as donor and acceptor moieties in FRET, which can be expressed in single cells or cell populations, adherent cells or in suspension, in a cell culture, a tissue culture, a mixed cell culture, a tissue explant, or in animal tissues in vivo, based on the teaching of Frommer, and further wherein the metabolite is lactate, and the metabolite binding protein is a bacterial LldR transcription factor, based on the combination of Aguilera and Frommer, and further wherein the bacterial LldR transcription factor having a sequence as the sequence disclosed by UniProt_P0ACL7, and suitable donor and acceptor fluorescent proteins moieties including donor and acceptor fluorescent proteins taught by Campbell and Miyawaki, respectively, in order to extend the teaching of Frommer to produce different metabolite nanosensors for monitoring different levels of metabolites including lactate by using protein sequences known in the art with expect success. Without a shared special technical feature, the inventions lack unity with one another.

Groups I-II therefore lack unity under PCT Rule 13 because they do not share a same or corresponding special technical feature.